Journal of Applied Volcanology

HAZARD MAP Open Access

# Ceboruco hazard map: part I - definition of hazard scenarios based on the eruptive history

Katrin Sieron[1*], Dolors Ferres[2], Claus Siebe[2], Lucia Capra[3], Robert Constantinescu[4], Javier Agustín-Flores[2], Karime González Zuccolotto[5], Harald Böhnel[3], Laura Connor[4], Charles B. Connor[4] and Gianluca Groppelli[6]

## Abstract

Of the 48 volcanoes in Mexico listed as potentially active by the National Center for Disaster Prevention (CENAPRED), Ceboruco, located in the western Trans-Mexican Volcanic Belt, is considered among the 5 most hazardous. Its recent eruptive history includes a large magnitude Plinian (VEI 6) eruption ~ 1000 years ago and the historical 1870–1875 vulcanian (VEI 3) eruption, as well as recent fumarolic and seismic activity.

Ceboruco is a relatively young (< 400,000 years) stratovolcano characterized by abrupt changes in eruptive behavior. Individual eruptive episodes have great variations in style (effusive andesitic to highly-explosive rhyodacitic) and duration. These factors complicate hazard assessment.

Three main eruptive scenarios of different magnitudes (large, intermediate, small) and eruption characteristics (likelihood of occurrence: high, medium, small) have been identified and will be presented as a background to build the volcanic hazard map for Ceboruco volcano (presented in part II of this work). Here, we report on the detailed eruptive history, with emphasis on the volcanic products of each of the eruptions, in order to identify those deposits that can serve as a reference for calibrating the modeling software (Tephra2 and Hazmap for ash fallout, Eject! code for ballistics, Etna Lava Flow Model for lava flows, Titan2D for pyroclastic density currents, and Flo-2D and LaharZ for lahars) that will be used in further steps to simulate different volcanic phenomena and lead to the construction of the hazard map.

**Keywords:** Ceboruco volcano, Hazard scenarios, Lava flows, Ash fallout, Ballistics, Pyroclastic flows and –surges, Lahars

## Introduction

Ceboruco volcano (21.75° latitude N and 104.30° longitude W, Mexico) is an active stratovolcano situated in the western part of the Trans-Mexican Volcanic Belt (TMVB) at the southern active margin of the North America plate (Fig. 1a). This volcano is considered the third most hazardous and of high risk in Mexico (Espinasa-Pereña et al., 2015; Espinasa-Pereña, 2018), due to its historical activity, its wide range of eruption styles (Sieron and Siebe, 2008; Sieron, 2009), previous impacts on pre-Hispanic settlements in the region (González-Barajas and Beltrán-Medina, 2013), and the current population density of ~ 55,000 people (INEGI, 2010 census) within a 10-km radius of the most recently active vent.

Important infrastructure nearby includes a federal toll road (No 15, Guadalajara-Tepic) cutting Ceboruco's N-flank, the freeway, the beltway to Puerto Vallarta, and the railroad (all located south of the volcano), as well as two of the most important hydroelectric power plants (both, 750 MW; 15% of total hydroelectric energy produced nationally; Comisión Federal de Electricidad, 2011) in Mexico: La Yesca and El Cajón, located along the Grande de Santiago river, 42 km to the E and 34 km to the N of Ceboruco's crater, respectively (Fig. 1b).

Ceboruco volcano is located in a particular geodynamic setting. Volcanism in this part of the TMVB has its origin in the subduction of the small Rivera plate and mostly involves evolved calc-alkaline magmas, although

* Correspondence: ksieron@uv.mx; ksieron@gmail.com
[1]Centro de Ciencias de la Tierra, Universidad Veracruzana, Lomas del Estadio s/n, Zona Universitaria, C.P. 91090 Xalapa, Mexico
Full list of author information is available at the end of the article

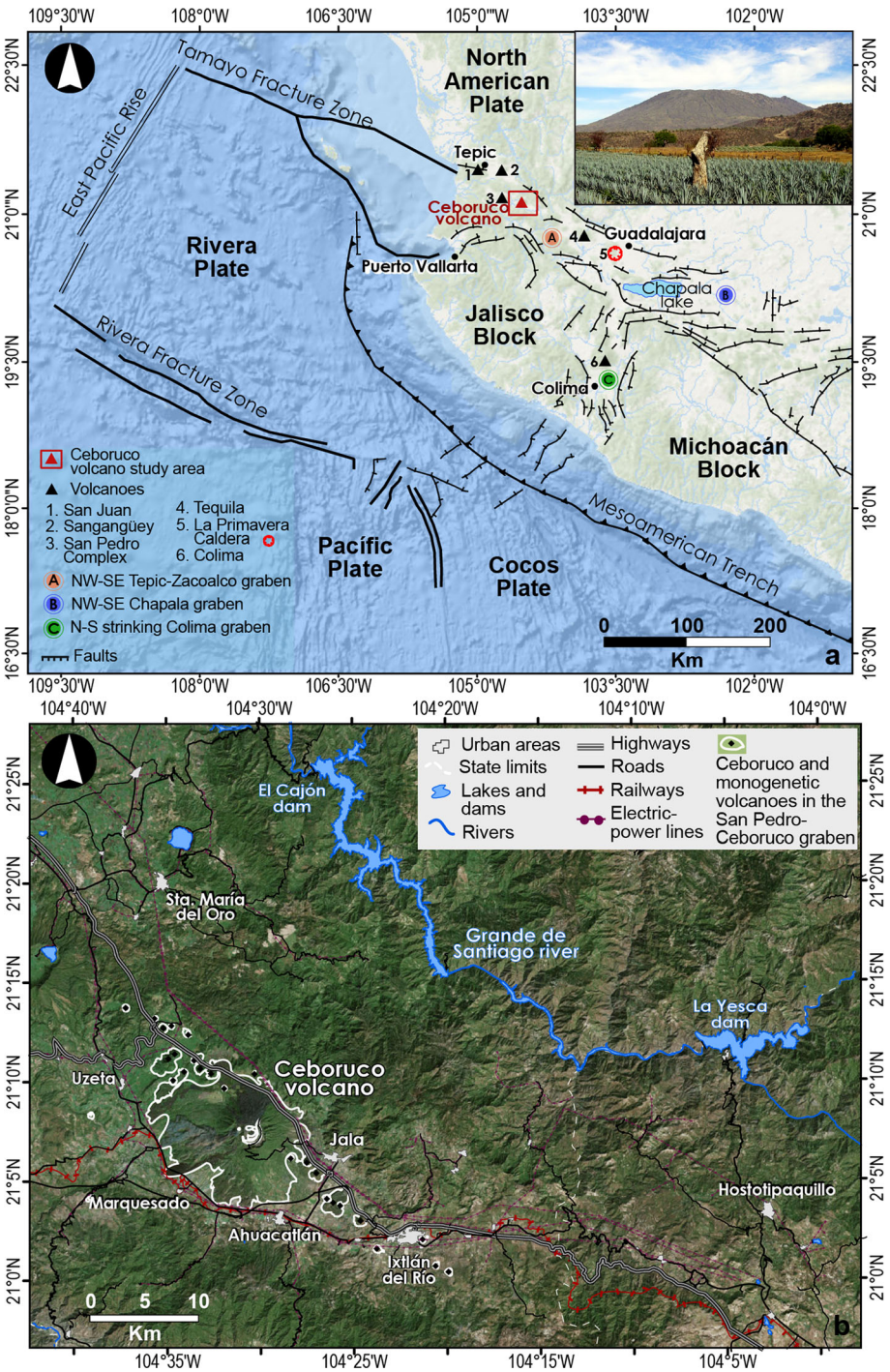


**Fig. 1** **a** Main tectonic features of the western TMVB and location of Ceboruco volcano in the TZ Graben **b** Google Earth base map, indicating infrastructure around Ceboruco and main dams along the Grande de Santiago River

subordinate alkaline mafic volcanism is also present (Ferrari et al., 1994, 2000a, 2000b, 2002, 2003; Petrone et al. 2001, Petrone, 2010). The subduction process has led to the formation of a regional tectonic structure, the Tepic-Zacoalco (TZ) graben, a complex system of individual grabens and horsts, within which dozens of monogenetic volcanoes and six polygenetic volcanoes occur (Fig. 1a). Specifically, Ceboruco volcano and ~28 monogenetic volcanic edifices sit within the San Pedro-Ceboruco half-graben (Petrone, 2010) (Fig. 1b and 2), at the northernmost sector of the TZ graben, along the boundary between the geologic units of the Jalisco Block (fault

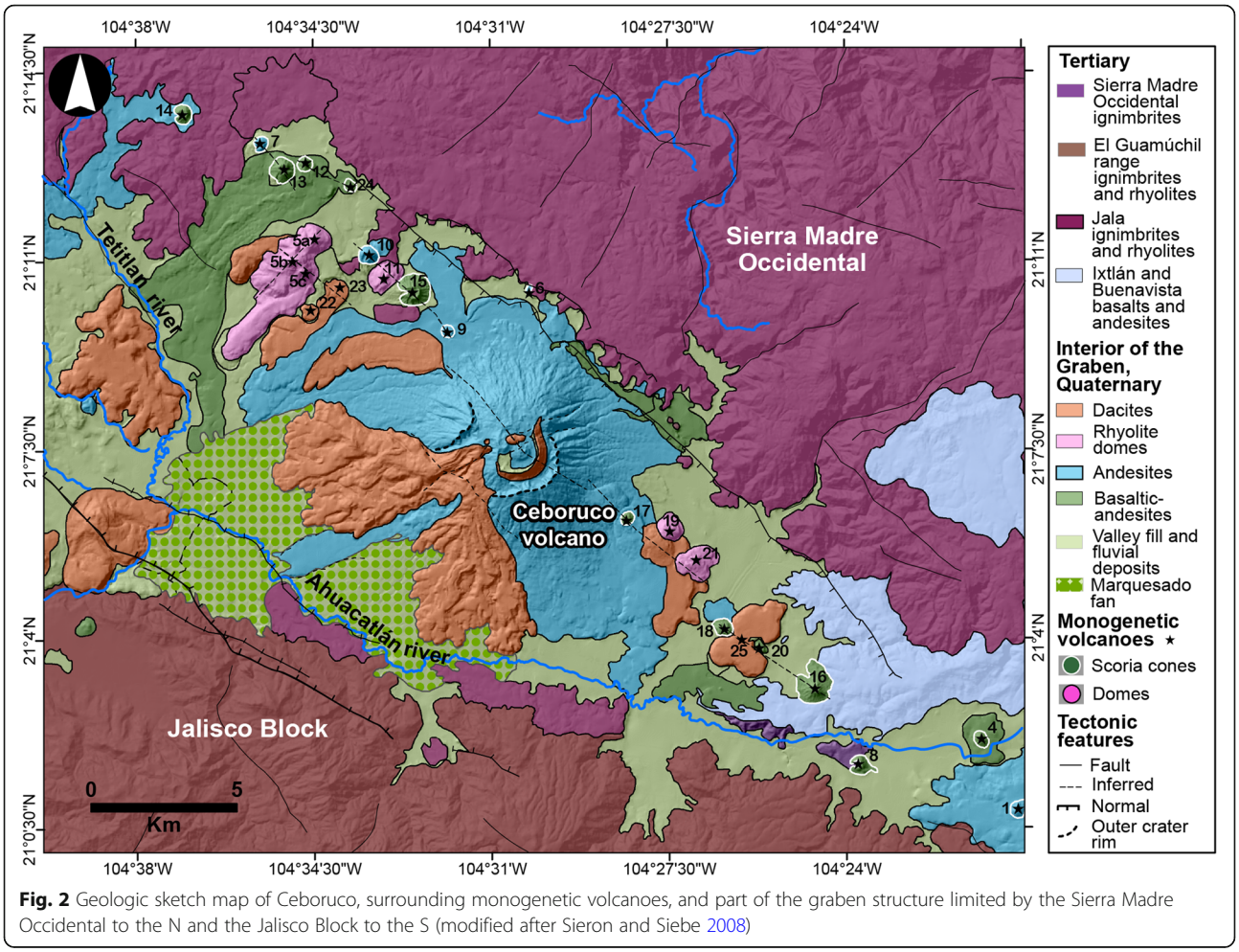


**Fig. 2** Geologic sketch map of Ceboruco, surrounding monogenetic volcanoes, and part of the graben structure limited by the Sierra Madre Occidental to the N and the Jalisco Block to the S (modified after Sieron and Siebe 2008)

bound part of the Guerrero terrane) and the Sierra Madre Occidental mountain range (Fig. 2).

The eruptive history of Ceboruco volcano includes a wide spectrum of effusive and explosive eruptions of different magnitudes (Nelson, 1986; Centro Nacional de Prevención de Desastres (CENAPRED), 2001; Gardner and Tait, 2000; Sieron and Siebe, 2008; Sieron, 2009), of which at least 8 occurred during the last 1000 years, including the Plinian Jala eruption radiocarbon-dated at 1, 060 ± 55 yr BP (Sieron and Siebe, 2008). These eruptions were characterized by the emission of lava flows, ash fall-out, ballistic projectiles, as well as pyroclastic surges and flows of different volumes (0.0025 to 1 $km^3$) and distributions. Also, syn-and-post eruptive lahars, as well as smaller gravity-driven mass movements form part of Ceboruco's eruptive sequences. The most recent eruption occurred CE 1870–75 and since then Ceboruco has experienced only minor fumarolic and seismic activity. Recent seismic studies indicate that although Ceboruco's activity is generally below background levels of other volcanoes, it presents a state of mild unrest (Rodríguez-Uribe et al., 2013). According to Sánchez et al. (2009) low frequency events indicate the presence of pressurized fluids or fluid-solid interaction and the excitation of trapped conduit waves. Furthermore, Rodríguez-Uribe et al. (2013) analyzed the same seismic dataset (i.e. 2003–2008) concluding that stresses could be increasing within the volcano. In addition, the volcano experienced a historical eruption in CE 1870–75 and has been extraordinarily active during the last 1000 years. All this indicates that an effort to assess volcanic hazards is needed. Other initiatives should also be undertaken (including closer geophysical surveillance, public awareness campaigns, etc.) in order to reduce volcanic risk in this region.

Although in recent years periodical seismic monitoring was conducted by the University of Guadalajara (Rodríguez-Uribe et al., 2013) and CENAPRED (Ministry of security and citizen protection), no permanent network exists. No comprehensive hazard map had been prepared until this research, even though the knowledge of Ceboruco's eruptive history was quite complete since Nelson's work in 1980 (Sieron, 2009).

As part of the project "*Evaluación del peligro volcánico del volcán Ceboruco (Nayarit) con énfasis en su*

*posible impacto sobre la infraestructura de la Comisión Federal de Electricidad"* (Volcanic hazard assessment of Ceboruco volcano (Nayarit), with emphasis on the possible impact on Federal Electricity Commission infrastructure), financed by the Comisión Federal de Electricidad (CFE), spatial hazard at Ceboruco is evaluated considering the different volcanic phenomena that may occur during future eruptions originating at the main volcanic edifice. In the present first part of this work, the eruptive history and the deposits associated with the eruptive activity are analyzed, in order to define the main future eruptive scenarios that could occur at Ceboruco volcano. In the second part (Sieron et al., 2019), the defined scenarios and volcanic reference deposits serve as a basis for computer simulations for each of the different phenomena (ballistics, tephra fallout, pyroclastic flows, and lahars) and results are presented together with hazard maps for the different scenarios envisaged. These individual hazard maps will then be integrated into the general hazard map for Ceboruco that will be made available to the public.

## The Ceboruco tectonic framework

The Ceboruco volcano is located in the San Pedro-Ceboruco asymmetric semi-graben, which is part of the larger NW-SE trending TZ graben, a large scale depression that together with the E-W oriented Chapala graben and the N-S Colima graben forms a triple junction in the vicinity of Guadalajara (Fig. 1a) (Luhr et al., 1985; Nieto-Obregón et al., 1992; Allan, 1986; Ferrari et al., 1994, 2000b, 2003; Rosas-Elguera et al., 1996).

The NE boundary of the Ceboruco semi-graben is marked by a normal NW-SE fault, which forms a prominent escarpment that separates the graben bottom from the reliefs of the Sierra Madre Occidental (Ferrari et al., 2002). Within the graben another important set of subordinate faults is inferred by the NW-SE alignment of several of the 28 monogenetic scoria cones and domes that occur in the vicinity of Ceboruco volcano, as well as by the morphology of escarpments observable at Ceboruco's main edifice (Fig. 2). The SW limit of the Ceboruco graben is marked by a successive southward elevation of the Jalisco Block, which forms the Sierra El Guamúchil, without clear evidence of another fault (Fig. 2). The graben is limited to the SE by a NNE-SSW striking fault.

Ceboruco is a truncated conical compound stratovolcano, with two concentric summit craters of 3.7 and 1.5 km in diameter respectively. One of the pyroclastic cones within the inner crater represents its highest peak reaching an elevation of 2164 m a.s.l. (above sea level), rising about 1000 m above the average surrounding valley floors. The main edifice is constituted by the superposition of lava flows and pyroclastic deposits that are mainly andesitic to dacitic in composition.

## Eruptive history of Ceboruco volcano

The construction of Ceboruco's edifice started in the late Quaternary (0.37 ± 0.2 Ma, Ferrari et al., 1997) and its eruptive history can be divided into two stages, separated by a prolonged period of inactivity (Nelson 1980). The first stage was predominantly effusive and led to the construction of the ancient cone (~ 370 ka to 45 ka (Ferrari et al., 1997; Frey et al., 2004) and the second stage (i.e. last 1000 years) is characterized by diverse eruptions including the explosive high-magnitude Plinian Jala eruption, responsible for the destruction of the main summit cone and its present morphology displaying a large caldera crater, and most of the voluminous pyroclastic deposits distributed throughout the area (Table 1).

### First stage of activity – ancient volcano

The oldest lavas do not crop out at the surface, but old lavas exposed at the summit caldera walls were dated by the K-Ar method at 0.37 ± 0.2 Ma (Ferrari et al., 1997). The initiation of Ceboruco's eruptive history occurred probably not much before that age as hinted by the limited thickness of Ceboruco lavas observed in the CFE-geothermal exploration drill hole (Ferrari et al., 2003). Accordingly, the construction of Ceboruco volcano started during the Late Pleistocene (see CB1-well drill core, Ferrari et al., 2003; Ferrari et al., 1997) with the predominantly effusive piling up of andesitic lava flows that successively built the main cone with a probable height of ~ 2700 m a.s.l (projecting the current flank angles towards a conical top) (Nelson, 1980, 1986). Average chemical composition of these lavas is 58.5 wt.% $SiO_2$, 17.8 wt.% $Al_2O_3$, and 5.8 wt.% total alkalis (Nelson, 1980; Sieron, 2009; Petrone, 2010). Lava flow morphologies (Aa and blocky) and associated breccias observed on the volcano flanks indicate that these lavas were emplaced at low viscosities. A volume of 40 $km^3$ (Nelson, 1986) was estimated roughly for the main cone and later determined more precisely to be 47 $km^3$ (Frey et al., 2004) by using an inclined base level and high-resolution ortho-photos (for more details see Frey et al., 2004; Sieron and Siebe, 2008).

Pyroclastic deposits associated to the first eruptive stage have not been found within the graben yet; the lowermost volcanic deposits on top of the Tertiary river conglomerates have their origin in the San Pedro dome complex and consist of pyroclastic sequences dated at 23,000 yr BP (Sieron and Siebe, 2008). On top of these San Pedro deposits, a paleosol is overlain by Ceboruco's 1,060 ± 55 yr BP Plinian Jala pyroclastic deposits (Sieron and Siebe, 2008).

**Table 1** Overview of the known eruptive history of Ceboruco volcano

| Stage | Phase | Ceboruco activity | Date or period | Products | Composition | Distance (km) | Magma volume ($km^3$) |
|---|---|---|---|---|---|---|---|
| 2nd stage of activity | Post-plinian | **VEI=3 historic eruption** | **1870-75** | Ash fallout | Trachy-andesite | ~30 (towards N and E) | 0.01 - 0.1 |
| | | | | Ballistic blocks | not found | does not apply | does not apply |
| | | | | Pyroclastic flows | not found (below 1870 lava flow) | ~2-5 km | <0.0005 |
| | | | | Lava flows | Trachy-Dacite | 7.7 | 1.14 |
| | | Lahars and erosion | | | | | |
| | | Phreatomagmatic and effusive activity within the inner Ceboruco crater (caldera) | **1060±55 years B.P.** (945-1022 CE) **- 1528** | Fallout of ash and pyroclasts Block- and ash flows Ballistic blocks Lava flows or lava domes | Andesite to dacite | 0.5-5 km? | |
| | | Effusive activity: N lava flows (probably associated explosive phases) | All post Plinian lava flows between **1,060-858 years B.P.** (1000-1142 CE) | Lava flow (**El Norte**) | Trachy-andesite | 4.2 | 0.36 |
| | | | | Lava flow (**Coapan II**) | Trachy-andesite | 12.4 | 0.31 |
| | | | | Lava flow (**Coapan I**) | Basaltic andesite | 6.8 | 0.08 |
| | | | | Lava flow (**Cajón**) | Trachy-andesite | 5 | 0.07 |
| | | Effusive activity: S lava flows (probably associated explosive phases) | | Lava flow (**Ceboruco**) | Trachy-andesite | 7.8 | 0.16 |
| | | | | Lava flow (**Copales**) | Trachy-Dacite | 7.03 | 2.11 |
| | | **Dos Equis** dome construction (and subsequent destruction and formation of the inner crater) | | Lava dome | Dacite | < 1 km | 1.3 (before destruction) |
| | **Plinian Jala Eruption** | **VEI=6 eruption**; Volume=3-4 $km^3$ (DRE); minimum affected area= 560 $Km^2$; opening of the outer Ceboruco crater | **1060±55 years B. P.** (945-1022 CE) | Pumice and ash fallout (towards NE) | Rhyodacite and dacite | >30 km | 2.7-3.4 (rhyodacite) + 0.2-0.3 (dacite) |
| | | | | Ballistic blocks | ? | 4.5 km | |
| | | | | Pyroclastic flows and -surges (N and S) | Rhyodacite and dacite | >20 km (N) and >10 km (S) | 0.09-0.12 (rhyodacite) + 0.04-0.05 (dacite) |
| | | | | Syn- and post-eruptive lahars | Heterolithologic | > 10 km (S) | |
| | | **Destiladero** lava flow | **1088-1060 years B.P.** (912-1505 CE) | Lava flow | Trachy-Dacite | 7.54 | 0.42 |
| Stage of inactivity (main edifice) | | | Thousands of years | Monogenetic Volcanism within Ceboruco graben | | | |
| 1st stage of activity | **Ancient volcano** | Dykes cutting the upper portion of the old edifice (today visible on the outer crater interior walls) | **45 ka** | | Andesite | - | - |
| | | **Main edifice lavas** | 0.37±0.2 Ma. (Ferrari et al.,1997) | Lava flow | Andesite | 8 km | ~45-47 (depending on shape of pre-Jala edifice considered) |

The latter observation supports the lack of deposition of pyroclastic deposits during the first stage of Ceboruco, rather than the loss of deposits due to erosion.

The end of the first eruptive stage (construction of the ancient cone) is based on the age of a lava dike corresponding to the youngest lavas exposed at the outer crater walls (Fig. 3) dated by Frey et al. (2004) at 45 ± 8 ka by the $^{40}Ar/^{39}Ar$ method.

## Repose of Ceboruco volcano and the monogenetic activity along the San Pedro-Ceboruco graben

The first stage of Ceboruco's cone construction was followed by a prolonged period of inactivity (after 45 ka) at the central edifice, as evidenced by the lack of deposits and lavas. Instead, deeply incised erosional gullies formed on its flanks and monogenetic activity occurred in its surroundings. Activity at the summit resumed shortly before 1000 yr BP (Fig. 3 and Table 1).

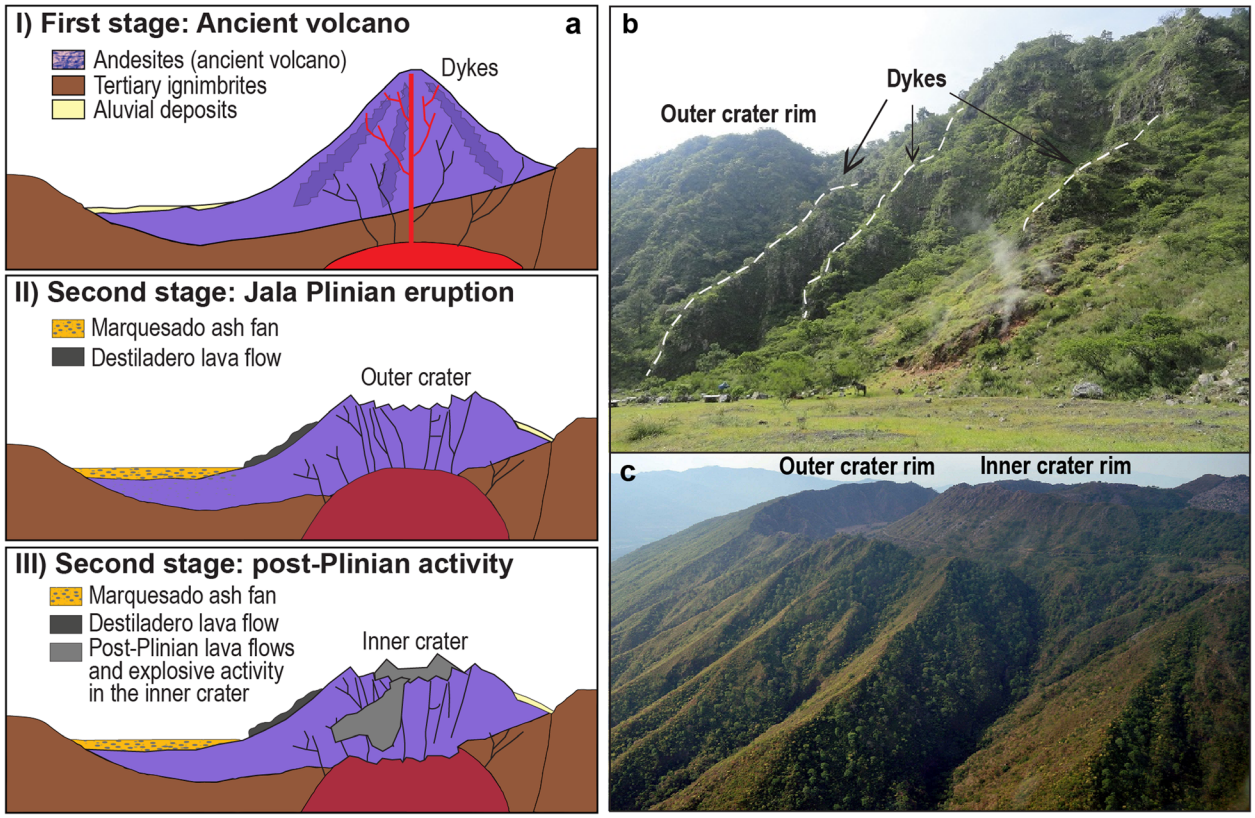


**Fig. 3** **a** Sketch illustrating the two main evolutionary stages of Ceboruco: I) First stage: Construction of the ancient volcano with a height of ~ 2700 m a.s.l. (after Nelson 1986); II) Second stage: Formation of the outer caldera crater during the Jala Plinian eruption, and III) Second stage: explosive activity and formation of the inner crater followed by effusive activity on the flanks leading to the present morphology of the volcano; **b** Photo showing the interior walls of the outer crater where dykes dated at 45 ± 8 ka (Frey et al. 2004) are exposed, and **c** Aerial photo taken from the NE showing the summit area, including the outer and interior crater rims

Monogenetic activity in the San Pedro-Ceboruco graben comprises at least 28 vents, 23 of them with ages ranging from ~ 100,000 to < 2000 yr BP. These small edifices are typically aligned in a NW-SE direction (Fig. 2 and Table 2) along faults parallel to the graben (Figs. 2 and 4). The alignment becomes also evident, when applying the kernel density function to individual vent locations, including small vents in Ceboruco's summit area and on its lower flanks (see Fig. 4).

Eleven monogenetic vents are < 12,000 yr BP and include 7 basaltic-andesite scoria cones and 4 silicic domes, which are either isolated or form small clusters. Two of them (Potrerillo II and San Juanito) initiated with brief phreatomagmatic phases producing a basal tuff ring around their vents (Sieron and Siebe, 2008). Construction of scoria cones was associated to Strombolian-type activity with moderate to low explosivity, while dome emplacement (e.g. Pochetero and Pedregoso) was generally characterized by initial magmatic explosive activity followed by effusive lava extrusion during the dome construction phase (Nelson, 1980; Sieron and Siebe, 2008).

Nelson (1980) analyzed the andesitic lavas of monogenetic edifices on the SE flanks of Ceboruco, and found that they do neither chemically resemble the pre-caldera andesites nor the post-caldera andesites of the main volcano. In this context, Petrone (2010) suggested that the magmatic systems of both, Ceboruco and the surrounding monogenetic volcanoes are related to each other and together produce the great chemical variety observable in Ceboruco's post-Plinian products. Further studies are necessary to understand the local magmatic system. Here we focus on the evaluation of volcanic hazards emanating from eruptions of Ceboruco's central volcano, and do not include those posed by monogenetic eruptions in its surroundings.

### Second stage of activity – the Jala Plinian eruption

After a long period of inactivity (about 40,000 years) at the central edifice, the dacitic Destiladero lava flow was

**Table 2** Monogenetic edifices of Ceboruco graben (individual numbers correspond to the ones in Fig. 2). Extended version of this table in Sieron and Siebe (2008)

| # | Type | Name | UTM x | UTM y | Age (ka) (exceptions are indicated) | Rock type | $SiO_2$ content (wt%) | Cone/Dome Height (m) | Cone volume ($km^3$) | Total volume ($km^3$) |
|---|---|---|---|---|---|---|---|---|---|---|
| 1 | Cone | Pedregal I | 568,019 | 2,323,749 | n.d. | Andesite | 57.90 | 80 | 0.01 | 0.01 |
| 2 | Cone | Pedregal II | 569,214 | 2,323,221 | n.d. | Andesite | 57.30 | 120 | 0.02 | 0.02 |
| 3 | Cone | Cerro Colorado | | | 430 ± 0.17 | Basalt | 52.00 | 60 | 0.009 | 0.009 |
| 4 | Cone | Cristo Rey | 566,819 | 2,326,220 | 403 ± 15 | Basaltic-andesite | 56.78 | 100 | 0.01 | 0.1 |
| 5 | Dome | *C. Grande* N | 544,005 | 2,343,272 | 111 ± 22 | Dacite | 67.9 (1) | – | – | – |
| | Dome | C. Grande M | 543,443 | 2,342,848 | | Rhyolite | 70.33 | – | – | – |
| | Dome | C. Grande S | 543,568 | 2,342,155 | | Rhyolite | n.d. | – | – | – |
| 6 | Cone | El Nogal | 551,351 | 2,341,451 | n.d. | n.d. | n.d. | 80 | 0.003 | 0.003 |
| 7 | Cone | Gavilán | 542,144 | 2,346,539 | 108 ± 22 | Andesite | 58.17 | 80 | 0.02 | 0.09 |
| 8 | Cone | Peña Colorada | 562,605 | 2,325,351 | 85 ± 19 | Basaltic-andesite | 54.09 | 100 | 0.02 | 0.02 |
| 9 | Cone | Molcajetito | 548,551 | 2,340,086 | n.d. | Andesite | 57.18 | 80 | 0.007 | 0.007 |
| 10 | Cone | C. de la Concha | 545,787 | 2,342,687 | 76 ± 18 | Andesite | 59.30 | 140 | 0.05 | 0.05 |
| 11 | Dome | Cerro Alto | 546,365 | 2,341,923 | 63 ± 7 | | 69.82 | – | 0.14 | 0.14 |
| 12 | Cone | La Tunita | 543,698 | 2,345,890 | n.d. | Basaltic-andesite | 53.54 | 80 | 0.01 | 0.01 |
| 13 | Cone | Los Amoles | 542,977 | 2,345,656 | ca. 57 ± 50 | Basaltic-andesite | 52.56 | 220 | 0.08 | 0.65 |
| 14 | Cone | Agujerado | 539,485 | 2,347,529 | ca. 34 ± 7 | Basalt | 51.90 | 120 | 0.02 | 0.12 |
| 15 | Cone | Molcajetillo | 547,352 | 2,341,468 | 12 ± 0.11 | Basaltic-andesite | 53.49 | 240 | 0.15 | 0.15 |
| 16 | Cone | Molcajete | 561,119 | 2,327,925 | 9.9 ± 0.17 | Basaltic-andesite | 54.00 | 240 | 0.13 | 0.23 |
| 17 | Cone | Ceboruquito | 554,677 | 2,333,668 | n.d. | Basaltic-andesite | 53.34 | 120 | 0.01 | 0.16 |
| 18 | Cone | Balastre II | 558,012 | 2,329,967 | n.d. | Basaltic-andesite | 55.74 | 100 | 0.02 | 0.032 |
| 19 | Dome | Pedregoso[b] | 556,159 | 2,333,296 | 3.55 ± 0.11 | Rhyolite | 70.81 | – | 0.2 (Do+C) | 0.41 |
| 20 | Cone | Balastre I | 559,220 | 2,329,324 | n.d. | Basalt | 51.69 | 80 | 0.005 | 0.005 |
| 21 | Dome | Pochetero[b] | 557,053 | 2,332,318 | 2.355 ± 0.11 | Rhyolite (Obsidian) | 74.14 | – | 0.14 | 0.14 |
| 22 | Cone | Potrerillo I | 543,866 | 2,340,845 | >Potrerillo II | Basaltic-andesite | 52.32 | 80 | 0.02 | 0.02 |
| 23 | Fm cone | Potrerillo II[a] | 544,880 | 2,341,636 | 2.34 ± 0.40 | Dacite | 64.37 | | – | 0.3 (Do+LF) |
| 24 | Fm cone | San Juanito[a] | 545,248 | 2,345,056 | 2 ± 31® | Basaltic-andesite | 54.39 | 80 | 0.01 | 0.01 |
| 25 | Dome | Pichancha Coulée | 558,605 | 2,329,611 | > 1.060 ± 55 and < 2.35 ± 0.11 AP | Dacite | 63.4 | – | – | 0.34 |

[a] combined edifice with outer tephra rim; [b]previous explosive magmatic phases; (1) $SiO_2$ content reported by Frey et al., 2004;® Frey et al., 2004; n.d.: no data

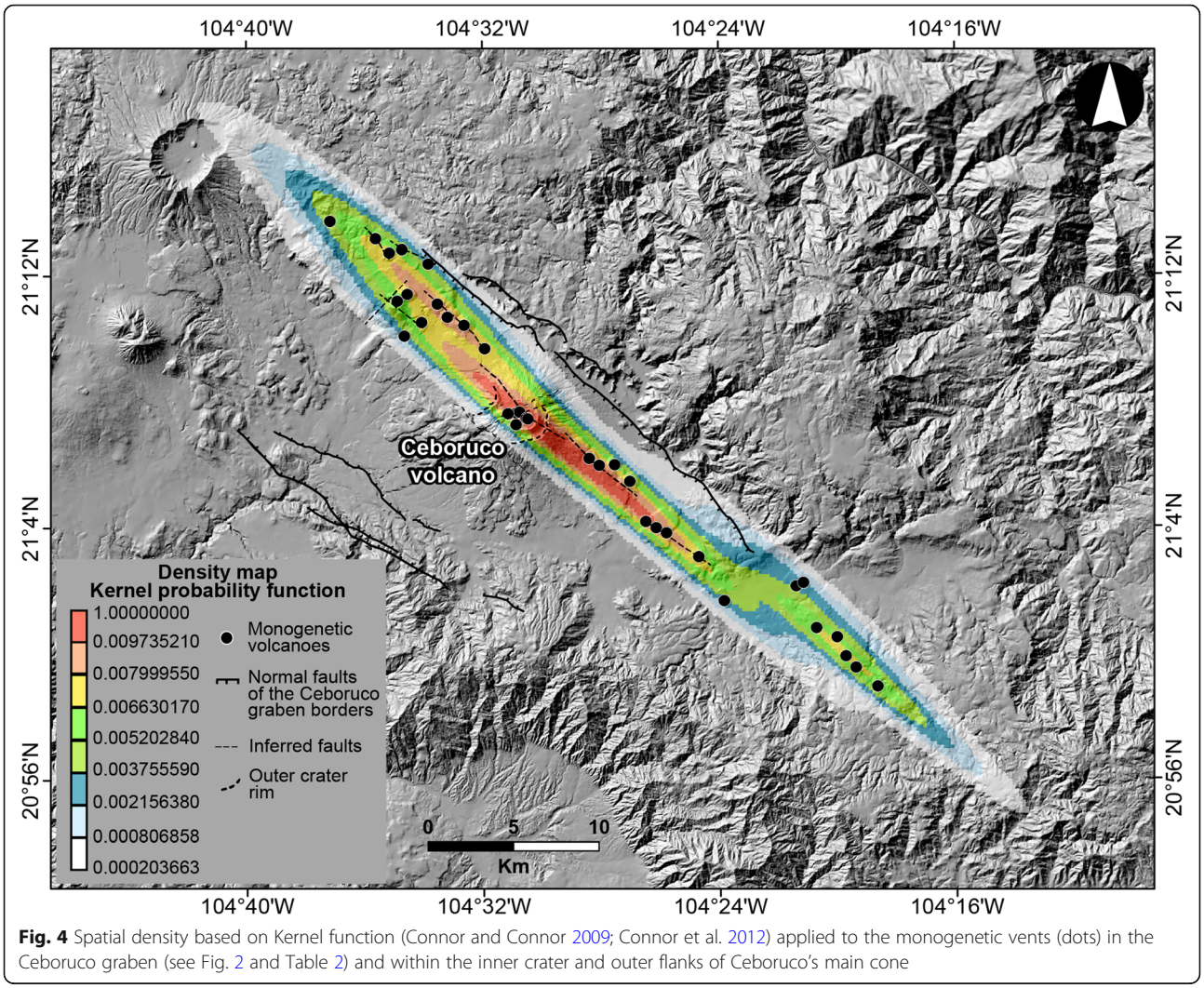


**Fig. 4** Spatial density based on Kernel function (Connor and Connor 2009; Connor et al. 2012) applied to the monogenetic vents (dots) in the Ceboruco graben (see Fig. 2 and Table 2) and within the inner crater and outer flanks of Ceboruco's main cone

emplaced on the WNW flank (Nelson, 1980; Sieron and Siebe, 2008). A total volume of 0.42 $km^3$ (Table 3) was determined through field data and using GIS software for the Destiladero lava flow, which marks a compositional change from purely andesitic lavas towards more evolved magmas. Sometime after its emplacement, the most violent eruption known from Ceboruco, the Plinian Jala eruption dated at 1060 ± 55 yr BP (Sieron and Siebe, 2008) took place. This eruption had a high volcanic explosivity index (VEI = 6; Newhall and Self, 1982), lead to the formation of the outer caldera with a diameter of 3.7 km, and produced extensive tephra fallout along the main dispersal axis towards the Sierra Madre Occidental, reaching well beyond the Grande de Santiago river, located 35 km to the NE and covering an area of > 560 $km^2$ with > 50 cm of pumice and ash (Nelson, 1980; Gardner and Tait, 2000). The greatest thicknesses of the deposits (up to 10 m) were found around Jala village, hence the name for this eruption (Fig. 5a).

The sequence of the individual eruptive phases and associated pyroclastic deposits of the Jala Plinian eruption were first described by Nelson (1980) and later by Gardner and Tait (2000), Chertkoff and Gardner (2004), and Browne and Gardner (2004, 2005) and includes 6 fallout layers, 4 pyroclastic flow, and 3 pyroclastic surge units. In summary, the eruption started with the rise of a 10-km-high eruptive column that produced a thin fallout deposit (P0) exposed in outcrops N of the vent (eruptive intensity of < $10^6$ kg/s; Gardner and Tait, 2000, using model of Carey and Sparks, 1986). Then, the thickest (up to 10 m) and most voluminous (8–9 $km^3$) pumice fallout unit (P1) was deposited mainly to the NE (Fig. 6a). During this phase, the column height varied between 25 and 30 km and the eruptive intensity between $4 \times 10^7$ and $8 \times 10^7$ kg/s.

**Table 3** Characteristics of Post-plinian lava flows of Ceboruco´s main edifice

| Lava Flow | Rock type | Area ($km^2$) | Thickness (m) | Maximun length (km) | Volume ($km^3$) |
|---|---|---|---|---|---|
| Destiladero | Trachy-dacite | 6.97 | 60 | 7.54 | 0.42 |
| Copales | Trachy-dacite | 23.69 | 80 | 7.03 | 2.11 |
| El cajón | Trachy-andesite | 7.07 | 10 | 5 | 0.07 |
| Coapan I | Basaltic-andesite | 4.04 | 20 | 6.8 | 0.08 |
| Coapan II | Trachy-andesite | 10.46 | 30 | 12.4 | 0.31 |
| El Norte | Trachy-andesite | 9.08 | 40 | 4.2 | 0.36 |
| Ceboruco | Trachy-andesite | 5.34 | 30 | 7.8 | 0.16 |
| 1870 | Trachy-dacite | 11.44 | 100 | 7.7 | 1.14 |

The main P1 phase was followed by a short period of quiescence, after which the P2 to P6 pyroclastic flow and surge units were deposited in various directions from the crater, but mainly towards the N and S with deposit-thicknesses ranging from a few cm (surges) to tens of m (pyroclastic flows) (Figs. 5a, 6b, and c). A main compound pyroclastic flow deposit thickness of up to 60 m is found towards the SW at quarries cut into the Marquesado block-and-ash fan located > 15 km from the crater. Surge deposits intercalated between fallout units were observed at distances of up to 20 km from their source (Figs. 5a and 6c).

The post-P1 phases together account for 25% of the total volume of the erupted magma. At the end of P1, caldera formation initiated, as evidenced by the considerable decrease in mass flow and the drastic increase in the lithic content compared to the main P1 fallout deposits (~ 8%) and post-P1 (30–60%), as well as in the change of magma composition (P1 = 98% rhyodacite, and post-P1 = 60–90% rhyodacite) (Gardner and Tait, 2000).

The total volume (DRE = dense rock equivalent) of the emitted material was estimated to be 3–4 $km^3$ (Nelson, 1980; Gardner and Tait, 2000), which suggests that this Plinian eruption was not only one of the most voluminous but also one of the most destructive (loss of vegetation, burial of pre-Hispanic settlements) eruptions in Mexico during the Holocene (Fig. 7).

All fallout deposits contain two pumice types, white rhyodacitic and grey dacitic, of which the first represents the overwhelming part of the total volume (2.8–3.5 $km^3$ of 3–4 $km^3$ DRE). According to Chertkoff and Gardner (2004) the magma is a mixture of three sources (bimodal mixture of rhyodacite and dacite, and a small component of basalt), that occurred in two stages: the mixing of dacite and basalt took place between 34 and 47 days, and the mixing between rhyodacite and dacite only 1–4 days prior to the eruption respectively (data obtained conducting zoning profiles in plagioclase and/or magnetite phenocrysts; see details in Chertkoff and Gardner, 2004). The Jala eruption is considered to be a small-volume caldera eruption according to Browne and Gardner (2004), during which lithics of successively shallower origin were expulsed: 6 km deep before the caldera collapse that produced the 3.5 km wide outer crater (the base of the P1 fallout unit contains < 15% lithics) and ~ 1 km deep during collapse (P1 unit contains up to 90% lithics toward its top).

Syn-and-post eruptive lahars, associated with the Jala eruption were mainly hyper-concentrated flows and fewer debris flows, distinguishable in the field, which reached distances of up to 10 km along the surrounding valleys, especially to the SW of the crater. The first were observed lying directly above Jala eruption pyroclastic flow deposits, while the latter are associated with valley fill and reworked material. The resulting lahar deposits are frequently intercalated with pyroclastic flow units on the N flank of Ceboruco, and occur predominantly in the upper section of the Marquesado block-and-ash fan to the S of Ceboruco (Fig. 2) in the case of the eruption-fed syn-eruptive lahars, and along the Ahuacatlán River (Fig. 5b) and surrounding plains in the case of secondary lahar deposits (Fig. 6d). Lahar units are also associated with the removal of the extensive fallout within the Sierra Madre Occidental close to Grande de Santiago river at 35–40 km N from Ceboruco, between the two hydro-electrical power plants La Yesca and El Cajón (Fig. 1b), although the deposits are poorly preserved or absent due to erosion on the steep slopes of the river canyon (only preserved in larger river loops).

Abundant archaeological remains found in the fertile valleys around Ceboruco indicate that the area has been inhabited at least since the Early Classic Period (CE 200–300) of the Mesoamerican archaeological time scale (Bell, 1971; Zepeda et al., 1993) by people belonging to the *Shaft Tomb*, *Cistón* (archaeologist José Beltran-Medina, personal communication), and *Aztatlán* cultural traditions (Barrera 2006; González-Barajas and Beltrán-Medina, 2013). Several of these settlements were buried underneath the Jala Plinian deposits as

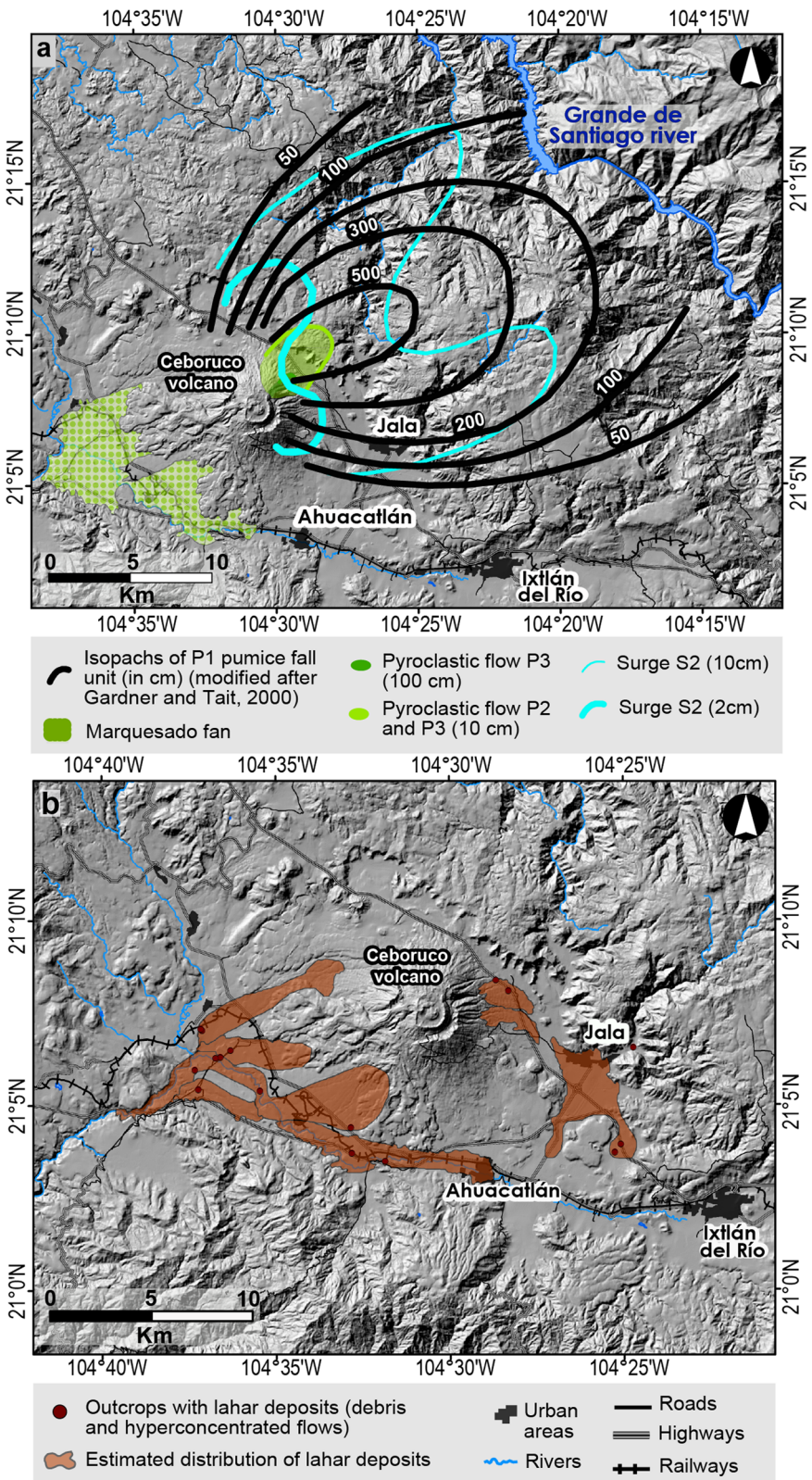


**Fig. 5** Maps showing the distribution of the Jala Plinian eruption deposits: **a** Distribution of P1 pumice fallout, surge, and pyroclastic flow deposits (modified after Gardner and Tait 2000) and **b** distribution of lahar deposits

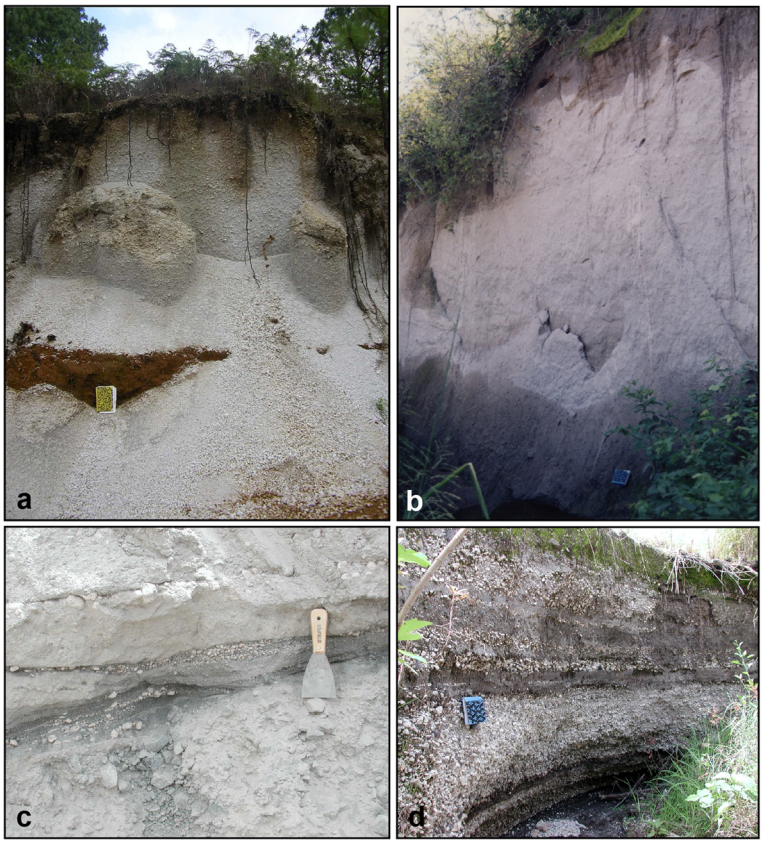


**Fig. 6** Photos of deposits produced by the Jala Plinian eruption: **a** P1 fallout, 16 km NE of the crater in the Sierra Madre Occidental area. **b** P2 pyroclastic flow deposit at roadcut between Uzeta and Las Glorias villages. **c** S2 surge unit at the Copales quarry to the SW of the crater. **d** Outcrop to the N of Ceboruco showing layers of pumice fallout overlain by a laharic sequence containing Jala pumice

evidenced by numerous tombs and household remains found by recent archaeological rescue excavations carried out during the construction of the new highway to Puerto Vallarta (González-Barajas and Beltrán-Medina, 2013).

## Post-Plinian effusive and explosive activity

The Jala Plinian eruption marks the beginning of a ~ 150-years-long period of intense activity at Ceboruco (Sieron and Siebe, 2008; Sieron et al., 2015; Böhnel et al., 2016) with the predominance of effusive lava flow

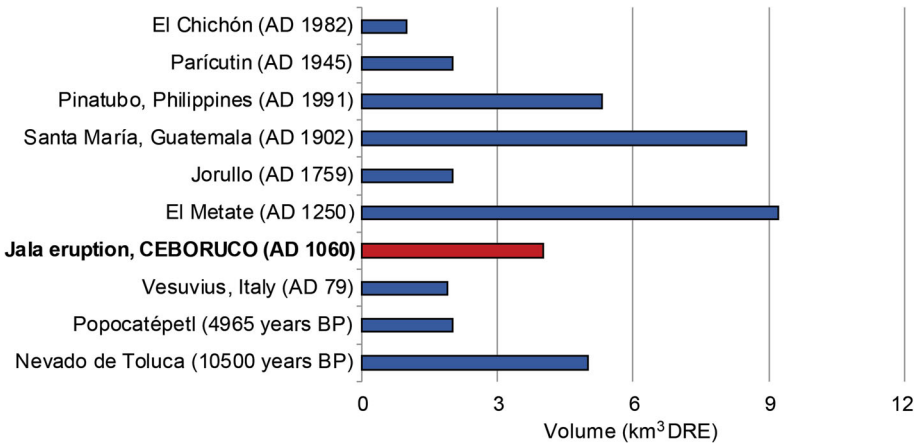


**Fig. 7** Volume-graph (DRE) of well-known Holocene eruptions in Mexico and elsewhere (after Chevrel et al. 2016). Note that the CE 1060 Jala Plinian eruption of Ceboruco volcano is among the most voluminous

emplacement and small explosive eruptions at the volcano summit area.

Shortly after the Jala Plinian eruption, the dacitic Dos Equis dome (Nelson, 1980; Sieron and Siebe, 2008) was emplaced in the caldera crater. This dome was laterally drained by the associated Copales lava flow (Fig. 8, Tables 1 and 2), also dacitic in composition (65–68.5 wt% $SiO_2$), which resulted in its deflation by subsidence, followed by its collapse and the subsequent formation of the inner crater of Ceboruco volcano (Nelson, 1980). Today, the remains of the Dos Equis dome form the margins of the inner crater and fragments are found in most post-Plinian lavas as xenoliths. The Copales flow inundated an area of 23.7 $km^2$ (Fig. 8) and has an average thickness of 80 m. Its total volume of ~ 2 $km^3$ makes it the most voluminous of all lava flows erupted during this period (Table 3).

After the emplacement of the Copales lava flow, five distinct mainly effusive trachy-andesitic (60–62 wt% $SiO_2$) eruptions produced the Cajón, Coapan I, Coapan II, El Norte, and Ceboruco flows (Sieron and Siebe, 2008; Fig. 8, Tables 1 and 2).

The post-Plinian lava flows on the N and SW flanks are almost completely covered by the remnants of the Dos Equis dome and shape the current morphology of the volcano. Although information from historical documents is lacking, and no pyroclastic deposits have been found associated to their eruptions, it is possible that the emplacement of some of these lava flows was accompanied by explosive activity producing minor ash that was subsequently removed by rain, as observed during and shortly after the historical 1870–75 eruption.

None of the post-Plinian lava flows could be dated by the radiocarbon method. Historical documents from the

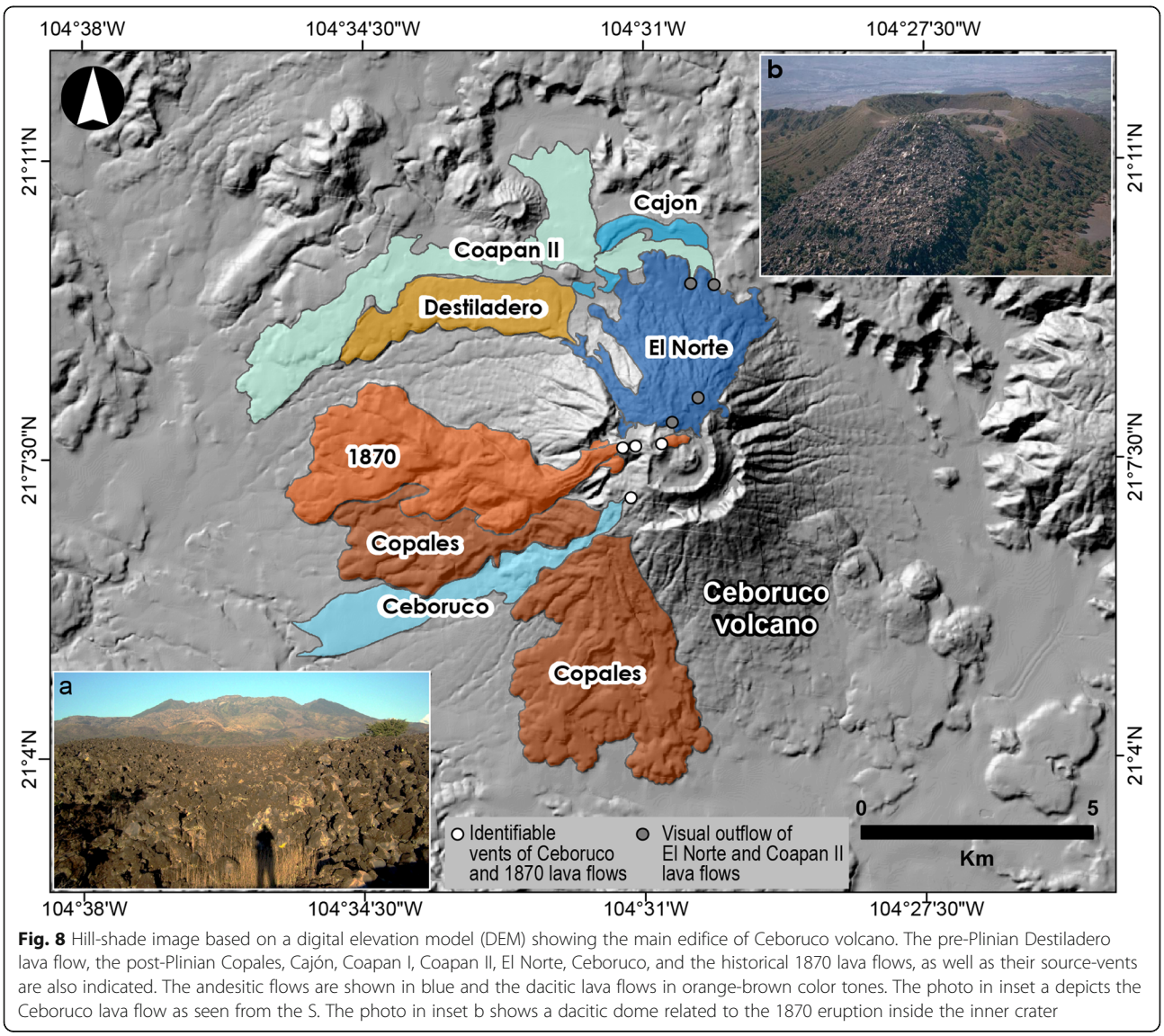


**Fig. 8** Hill-shade image based on a digital elevation model (DEM) showing the main edifice of Ceboruco volcano. The pre-Plinian Destiladero lava flow, the post-Plinian Copales, Cajón, Coapan I, Coapan II, El Norte, Ceboruco, and the historical 1870 lava flows, as well as their source-vents are also indicated. The andesitic flows are shown in blue and the dacitic lava flows in orange-brown color tones. The photo in inset a depicts the Ceboruco lava flow as seen from the S. The photo in inset b shows a dacitic dome related to the 1870 eruption inside the inner crater

time of the Spanish conquest reveal that for the exception of the 1870 lava flow, all other post-Plinian lava flows already existed by the time of the Spaniard's arrival to the study area in CE 1528 (Ciudad Real, 1976; Arregui, 1946). Stratigraphic relationships indicate the order of the effusive eruptions on Ceboruco's flanks: Cajón, Coapan I, Coapan II, and Norte to the N; and Copales, Ceboruco, and 1870 to the SW.

Because of morphological differences between the different lava flows, Sieron and Siebe (2008) hypothesized that the 6 lava flows (excepting the 1870 flow) were emitted in sequence, one after the other, and separated by short periods of relative quiescence over a total time interval of ~ 500 years from CE ~ 1000 (shortly after the Jala eruption) to CE 1528 (arrival of the Spaniards). This previous assumption turned out to be incorrect, as discovered recently by a secular variation paleomagnetic study (Böhnel et al., 2016). Surprisingly, all six lava flows (total volume of ~ 3 $km^3$) were emitted during a short period of only ~ 140 years between CE ~ 1000 and CE ~ 1140 (Böhnel et al., 2016), briefly after the Plinian Jala eruption and much before the arrival of the Spaniards in 1528 (Figs. 9 and 10). This short period of activity is followed by 700 years of relative quiescence interrupted by the historical eruption of 1870–1875 (Fig. 10). The minor eruptions at the summit area that gave rise to the small pyroclastic cones and domes nested within the inner caldera were probably contemporaneous to the post-Plinian lava flows. Volcanic constructs inside the caldera include dome complexes and pyroclastic cones: El Centro dome, which might be contemporaneous to El Norte lava flow (their chemical composition is almost identical); Pyroclastic Cone I located in the NW sector of Ceboruco's inner crater, which currently holds the highest altitudinal point of the entire volcano (La Coronilla); and Pyroclastic Cone II near the SW margin of the inner crater. All these constructs were formed along a zone of weakness and are aligned in a WSW-ENE direction. Thus, during the first two centuries after the Jala Plinian eruption, not only voluminous lava flows were produced (see preceding paragraphs), but also smaller explosive eruptions occurred within the summit crater. Deposits associated to the three structures (two pyroclastic cones and one pyroclastic ring surrounding a lava dome) within the interior crater mentioned above offer evidence (e.g. pyroclastic surge deposits and breadcrust bombs) pointing to the presence of water that resulted in brief phreatomagmatic phases during their explosive-magmatic emplacement (Sieron and Siebe, 2008).

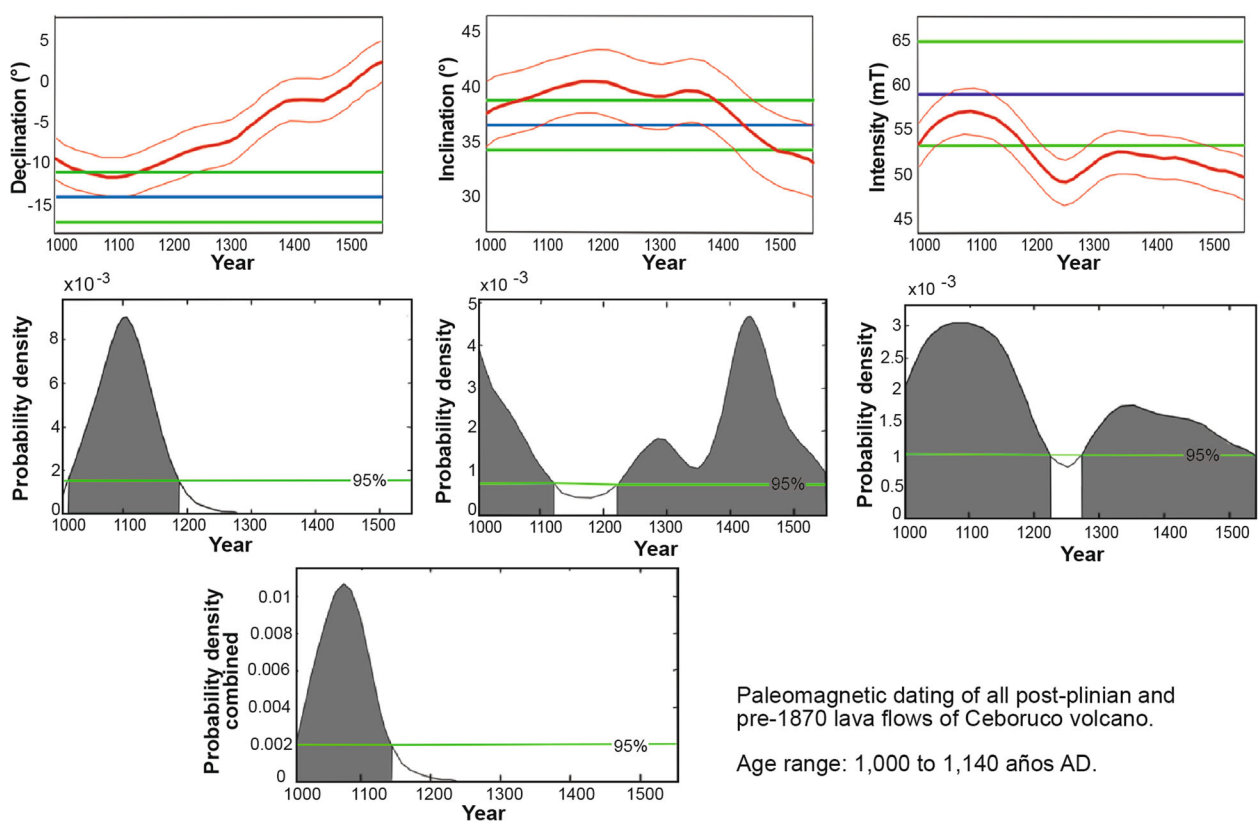


**Fig. 9** Paleomagnetic dating of all post-Plinian and pre-1870 Ceboruco lava flows (from Böhnel et al. 2016)

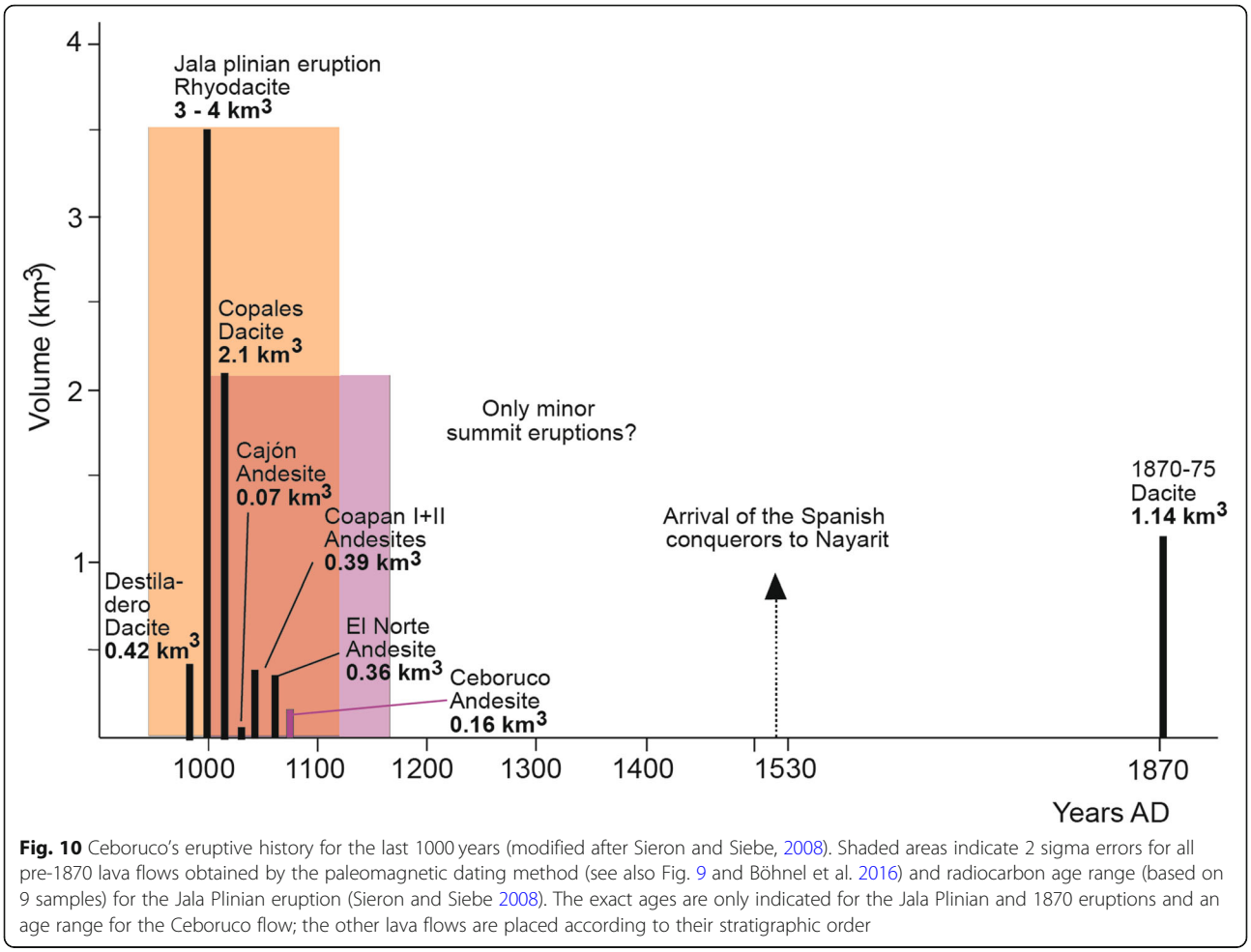


**Fig. 10** Ceboruco's eruptive history for the last 1000 years (modified after Sieron and Siebe, 2008). Shaded areas indicate 2 sigma errors for all pre-1870 lava flows obtained by the paleomagnetic dating method (see also Fig. 9 and Böhnel et al. 2016) and radiocarbon age range (based on 9 samples) for the Jala Plinian eruption (Sieron and Siebe 2008). The exact ages are only indicated for the Jala Plinian and 1870 eruptions and an age range for the Ceboruco flow; the other lava flows are placed according to their stratigraphic order

The total volume of post-Plinian lava flows was first estimated by Nelson (1980) at 7 $km^3$, later by Frey et al. (2004) at 9.5 $km^3$, and finally by Sieron and Siebe (2008) at 4.4 $km^3$ with individual lava flows varying between 0.07 and 2.1 $km^3$ (Table 3). Differences in these estimates are mainly related to the quality (resolution) of available topographic data and derived digital elevation models and/or images used for interpolating individual outlines of the lava flows, many of which are partly covered by subsequent younger lavas.

Estimated volumes indicate high eruption rates of 0.004 $km^3$/year (Sieron, 2008). Extrapolation of such high eruption rates to the pre-Jala stage would imply an unrealistically fast construction of the main edifice in only 4000 years (using a total volume of 38 $km^3$ estimated by Frey et al., 2004), or 8800 years (using a value of 60 $km^3$, as estimated by Nelson 1980) or 11,500 years (using 46 $km^3$, as estimated by Sieron and Siebe 2008). Although quite different, all these estimates are within the same order of magnitude. Since the youngest dated dykes are 45 ± 8 ka old (Frey et al., 2004; see also Fig. 3), it is clear that prolonged periods of repose must have occurred and that eruption rates must have varied considerably during Ceboruco's eruptive history.

### The historical 1870–1875 eruption and recent activity

The most recent eruption of Ceboruco took place in 1870–1875 and its magnitude has been ranked with a VEI = 3 by the Global Volcanism Network program (Global Volcanism Program (GVN), 2017, Smithsonian Institution). Caravantes (1870) and Iglesias et al. (1877) visited Ceboruco at that time, and described the entire course (1870–75) of the eruption based on their own observations (see also Palacio, 1877). In addition, they obtained information from the inhabitants of the adjacent towns such as Ahuacatlán and Jala (Barrera, 1931; Banda, 1871). Based on the publications of Caravantes (1870) and others, additional information was published in Germany by Kunhardt (1870) and Fuchs (1871). Sieron and Siebe (2008) provide an extensive discussion of the original observations; here we only present a summary of the main characteristics of this eruption.

Early signs of unrest were reported in 1783 and 1832 and included underground noise, seismic activity, and the

observation of a whitish vapor plume emanating from the volcano's summit area. In 1832, these premonitory phenomena were felt strong enough to cause fear among the inhabitants of neighboring Jala, who abandoned their homes for a few days (Iglesias et al., 1877). Several decades later, unrest resumed and reached again higher levels. The exact timing of the peak of premonitory unrest in 1870 varies from author to author, but occurred between the 15th and 21st of February, shortly before the beginning of the eruption on February 23, 1870, which lasted until 1875, when "small eruptive columns loaded with ash were still rising at intervals of 10 minutes" and the lava flow was still moving slowly (García, 1875; Iglesias et al., 1877).

At the beginning of the main phase of the eruption, pyroclastic flows and surges travelled down the ravines on the southern slope (Caravantes, 1870; Lacroix, 1904; Waitz, 1920). Caravantes (1870) describes fresh pyroclastic deposits in the Los Cuates ravine and the advancement of an 80-m-high viscous lava flow front through this same ravine (Fig. 11a).

Ash fallout visibly covered the landscape up to 15 *leagues* (~ 85 km) from the crater and thicknesses of up to 50 cm were observed (Banda, 1871). In 1872 the main lava flow ceased to advance, but vertical inflation was still observed (Iglesias et al., 1877) and new lava emerged along several fractures higher up on the SW flank, as well as inside the inner summit crater. In Guadalajara and other parts of the State of Jalisco seismic activity was felt during several periods during the course of the eruption, and one peak is reported for the first months of 1875.

The eruption formed a small crater to the W of Pyroclastic Cone I, inside the inner crater (Fig. 11b). This activity partially removed the rim of the W crater of Pyroclastic Cone I, becoming now the E margin of the new 1870 crater, where a dome is present today (Fig. 11c and d).

Sieron and Siebe (2008) and Sieron (2009) determined the total volumes of the 1870–75 eruptive products. A volume of ~ 1.14 $km^3$ was calculated for the lava flow (Table 3) and a maximum of ~ 0.1 $km^3$ for the ash fallout deposits (Fig. 12a and b). The volume of the pyroclastic flows and surges associated with this eruption is much smaller (~ 0.0005 $km^3$).

The ash deposits are fine-grained (Fig. 13a) and have been exposed at the surface for more than a century (Fig. 12). As a result they have been partly eroded and are not identifiable at many places, especially in distal areas. Based on the observations reported by Banda (1871) we estimated that an area of 400 to 500 $km^2$ must have been affected by the 1870–75 ash fallout with thickness ranging between a few mm and 50 cm.

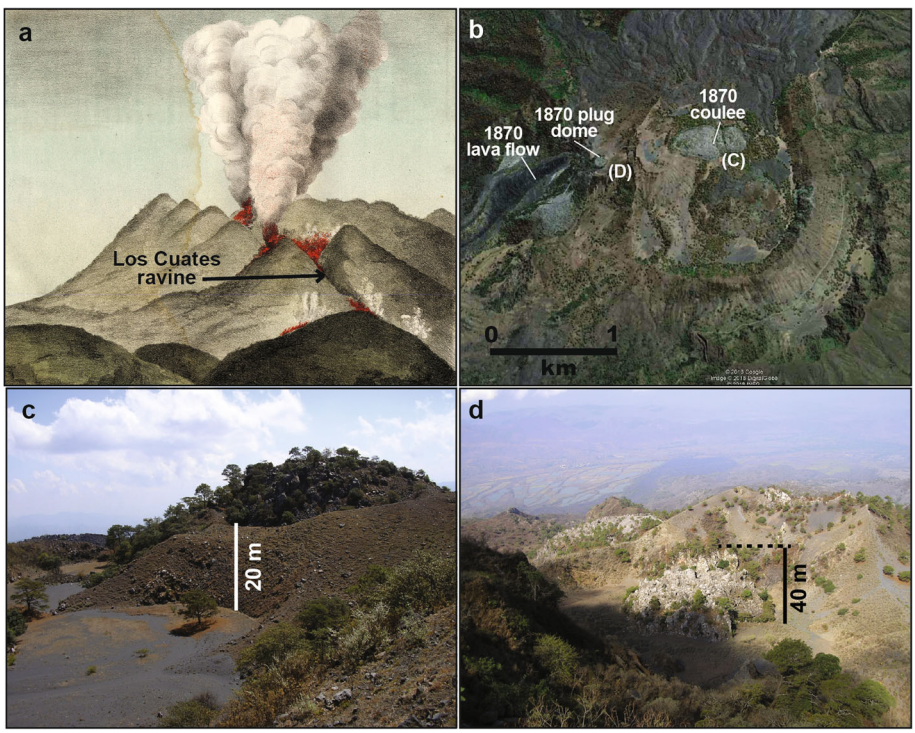


**Fig. 11** Features of the 1870–75 eruption. **a** Painting by a witness of the 1870 eruption (from Banda 1871; unknown artist). **b** Google-Earth satellite image of the crater region, where features shown on photos C and D are indicated (see Sieron and Siebe 2008, for geologic interpretation). **c** Pyroclastic cone and 1870 ash covering the adjacent plain and to the right part of the 1870 dome-coulee. **d** 1870 crater with small dome (foreground) and 1870 lava flow (background)


**Fig. 12** Ash fallout deposits produced by the 1870–75 eruption: **a** 1870 ash covering the Plinian Jala pumice at the lower eastern Ceboruco flanks, 6 km from the crater. **b** 1870 ash covering reworked Plinian deposits at roadcut along the new highway to Puerto Vallarta on the south flank of Ceboruco

The chemical composition of the 1870–75 products varies from andesite (ash fallout) to dacite (domes and lava flow) (Fig. 13b) and the eruption style of the activity can be labeled as vulcanian for the most part of this period of time.

After 1875, fumarolic activity and occasional small ash plumes persisted for another 5 years (Iglesias et al., 1877; Ordóñez, 1896). By 1894 (almost 20 years after the cessation of the main eruption), two major fumaroles were still active within the 1870 crater with temperatures of 96 °C, and additional fumaroles were visible along the 1870 lava flow (Ordóñez, 1896). Since then, fumarolic activity has gradually diminished but persists until today. Low-temperature fumaroles occur at the SE inner crater wall of the outer caldera (1952 m a.s.l.; Fig. 14a and b) and at the foot of one of the small 1870 plug-domes within the inner crater (Fig. 14c and d).

CENAPRED has conducted a monitoring campaign of fumaroles and springs in recent years (since 2005). In 2015, temperatures of 80 °C at the outer caldera fumarole site

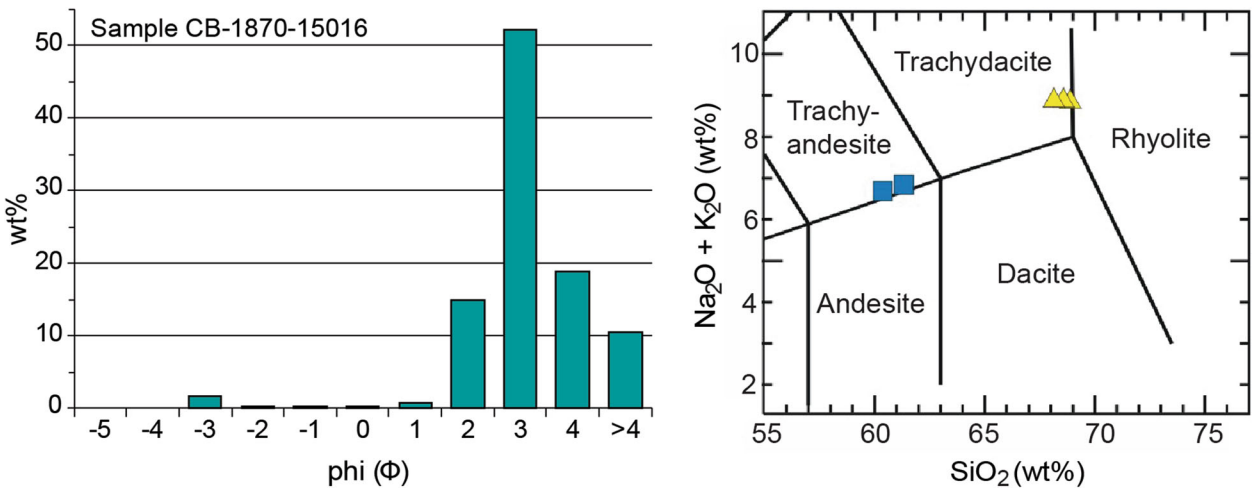


**Fig. 13** Left: Grain-size distribution of the CE 1870 ash fallout collected on Ceboruco's northern flank. Right: Total alkalis vs. silica (TAS) diagram (LeBas et al. 1986) of analyzed samples from lavas and domes (yellow triangles) and of the CE 1870 ash (blue squares)


**Fig. 14** Present fumaroles at Ceboruco volcano. **a** and **b**: Base of inner wall of outer caldera crater. Photos taken January 2016 by Claus Siebe. **c** and **d**: Base of the 1870 plug-dome within the inner crater; photos taken in 2015, courtesy of CENAPRED

and of 84 °C at the inner crater plug-dome (Fig. 14c and d) were measured. In addition, six springs were repeatedly sampled for chemical analysis at the base of the volcano within the basin of the river Ahuacatlán. So far, temperatures and chemical compositions of fumaroles and spring waters have remained within a narrow base-line range, ruling out magmatic reactivation (CENAPRED, 2016).

A permanent seismic monitoring network does not exist at Ceboruco. The University of Guadalajara and the Civil Protection Office of the State of Nayarit installed a temporary (2003–2008) seismic station (CEBN) on the south flank of the volcano (2117 m a.s.l.). Sánchez et al. (2009) and Rodríguez-Uribe et al. (2013) classified the seismicity recorded within a radius of 5 km around the seismic station into three major types of events following the scheme proposed by McNutt (2000): a) Volcano-tectonic earthquakes (VT), which indicate a stress propagation regime in the faults that cross the volcanic edifice at a low but consistent rate; b) low frequency earthquakes (LF), which might be related to the presence of pressurized fluids or to fluid-solid interaction; and c) mixed or hybrid events, which are signals derived from processes close to the surface that might indicate renewed or intensified fumarole activity in or near the plug-domes in the interior crater, consistent with an active hydrothermal system.

The increase in the seismic activity suggested by these studies (Sánchez et al., 2009; Rodríguez-Uribe et al., 2013) is based on a limited set of data (only one station, few years of recording) and needs to be viewed with caution. Nonetheless, it represents a valuable attempt to determine the level of base-line activity at Ceboruco and compares successive events in a time frame of 5 years. Furthermore, it underscores the need to implement a more extensive monitoring network that would allow clarifying Ceboruco's current state of activity, and make a more thorough hazard assessment.

## Volcanic hazard assessment of Ceboruco volcano and proposed hazard scenarios

### Interpreting the eruptive history

As outlined earlier, Ceboruco is a young historically active stratovolcano, which initiated activity in the Late Pleistocene. Mostly andesitic effusive eruptions characterized the first stage of edifice construction. Then, after a long period of repose, more silicic activity culminated in the violent VEI 6 rhyo-dacitic Plinian Jala eruption followed by a voluminous post-Plinian stage (6 eruptions in 150 years) with evident magma mixing processes producing moderately violent dacitic and more effusive andesitic eruptions. It is a common observation that longer repose periods at stratovolcanoes may lead to magma evolution and to more violent eruptions. Nonetheless, a clear eruptive pattern is not discernible and Ceboruco's future behavior is hence not predictable.

In conclusion, eruptions have shown a great diversity of styles since the beginning of Ceboruco's history. A great variety of volcanic processes took place during these eruptions (Table 4), posing different levels of

**Table 4** Volcanic deposits found in the Ceboruco stratigraphic record associated with different volcanic phenomena

| Volcanic phenomena | Eruptive record | | Data of Ceboruco volcanic deposits | | | | | Deposits of reference for simulations |
|---|---|---|---|---|---|---|---|---|
| | # | Events | Units | Axis distribution | Lengths (km) | Area ($km^2$) | Thickness | |
| Tephra fallout | 7 | 1870 eruption | 1 | NE | | 400 | > 10 cm | 1870 ash fall |
| | | Jala Plinian eruption | 6 | NE | | 560 | > 50 cm | P1 unit |
| Lava flows | 8 | Andesitic composition | 5 | all directions (N-W-S) | 4–12 | 5.3–10.5 | 10 m - 40 m | Ceboruco lava flow |
| | | Dacitic composition | 3 | | 7–7,7 | 7–23 | 60 m - 100 m | 1870 lava flow |
| Pyroclastic flows | 4 | Jala Plinian eruption | 4 | N and SW | > 15 | | cm to m | P2 and P3 units |
| Pyroclastic surge | 4 | Jala Plinian eruption | 3 | N and SW | up to 20 | | cm | S2 unit |
| | | 1870 eruption | 1 | N-NE | ~ 1 | | cm | S3 unit (Jala eruption) |
| Lahars | 4 | Hyperconcentrated | 3 | N and SW | up to 10 | | cm to m | All deposits (volume of main units) |
| | | Debris-flows | 1 | N and SW | | | cm to m | |

hazard and risk to the surrounding areas. The three main hazard scenarios described in the next section encompass all observed eruption styles, varying from merely effusive andesite eruptions (scenario of small magnitude) which statistically is the most probable scenario (ancient cone lavas and modern andesite lava eruptions), to moderately explosive dacite eruptions (scenario of intermediate magnitude) as observed during the 1870 historical eruption, up to violent Plinian eruptions (scenario of large magnitude). Only one Plinian eruption (Jala) has been registered during the entire eruptive history of Ceboruco volcano. It represents the least probable, but most destructive type of eruption to occur again in the near future.

## Volcanic phenomena expected from future eruption

Ceboruco's stratigraphic record reveals many types of deposits, including lava flows, tephra fallout, ballistic ejecta, pyroclastic flows and surges, and lahars (Tables 1 and 4).

The most common type of activity in the past and hence expected to most likely occur during future eruptions consists of andesitic lava flow emission accompanied by minor explosive activity, as was typical for the first cone-constructing phase and also on several occasions during the past 1000 years of its eruptive history. The second most common type of eruption comprises the emission of more evolved dacitic magmas (e.g. Dos Equis dome, Copales, and 1870 lava flows). These eruptions were accompanied by explosive activity (fallout, pyroclastic flows and surges).

## Definition of hazard scenarios

Based on the eruptive history, three main hazard scenarios were defined for Ceboruco volcano (Table 5). Each scenario is characterized by a likelihood of occurrence (high, medium, low) and is associated with an eruption magnitude (small, intermediate, and large). For instance, the highest likelihood of occurrence (scenario 1) corresponds to eruptions of minor magnitude. Such eruptions would affect relatively small areas, but would occur frequently. The lowest likelihood of occurrence (scenario 3) comprises Plinian eruptions of the largest magnitude that would severely affect vast areas.

### *Scenario 1 (low magnitude, VEI < 2)*

Effusive eruption of andesitic composition involving 0.02 to 0.5 $km^3$ of magma similar to the Cajón, Coapan I and II, Norte, and Ceboruco lava flow emissions (Fig. 8). This type of eruption would produce one or more lava flows, probably accompanied by a low magnitude explosive phase with the emission of ash and ballistic fragments from 1 to 5 km-high eruptive columns. The eruption could originate within the central crater or from a vent at the flanks of the volcano (most probably N and SW flanks). The major part of the involved magma volume would be emitted as part of a lava flow and only a minor portion as pyroclastic materials. Lahar generation is not considered in this scenario.

### *Scenario 2 (intermediate magnitude, VEI 2–3)*

Explosive Vulcanian-style eruption of minor to moderate magnitude, including effusive phases. Magma composition would be most likely dacitic with volumes varying between 0.5 and 2.5 $km^3$, as observed during the historical 1870–75 eruption. The explosive phases of this type of eruption would include eruptive columns of 5 to 15 km in height producing ash (tephra) fallout and ballistic fragments, as well as pyroclastic flows and surges. Dacitic lava flows could be emitted from the central crater or flanks. Lava dome formation would be probable due to the high viscosity of the dacitic magmas and lava flows would reach shorter distances than in *scenario 1*. The greater amount of emitted pyroclastic materials (compared to *scenario 1*) would create conditions for lahar formation during and after the eruption.

**Table 5** Hazard scenarios defined for Ceboruco volcano. The processes involved in each eruptive scenario are indicated

| Scenarios | Description | Volcanic phenomena | | | | |
|---|---|---|---|---|---|---|
| | | ASH FALLOUT | BALLISTIC BLOCKS | LAVA FLOWS | PYROCLASTIC FLOWS | LAHARS |
| SCENARIO 1 | Effusive eruption of andesitic composition Volume: 0.02–0.5 $km^3$ Eruptive column height: 1–5 km VEI < 2 | Volume | Diameter | Volume | | |
| | | 0.001–0.025 $km^3$ | 0.1–0.5 m | 0.02–0.475 $km^3$ | | |
| | | Eruptive column height | Density | Average thickness | | |
| | | 1–5 km | Andesite 2500 $kg/m^3$ | 10–40 m | | |
| | | Granulometry | Initial velocity | Length | | |
| | | Samples of 1870 eruption | 150 a 200 m/s | 8–15 km | | |
| SCENARIO 2 | Vulcanian eruption, with a dacitic effusive phase Volume: 0.5–2.5 $km^3$ Eruptive column height: 5–15 km VEI: 2–3 | Volume | Diameter | Volume | Volume | Volume |
| | | 0.05–0.25 $km^3$ | 0.1–0.5 m | 0.475–2.125 $km^3$ | 0.025–0.125 $km^3$ | 0.5–3/4 x $10^6 m^3$ (water + sediments) |
| | | Eruptive column height | Density | Average thickness | Bed friction | Sediment input areas |
| | | 5–15 km | Andesite/Dacite 2500–2800 $kg/m^3$ | 40–140 m | | Ceboruco slopes |
| | | Granulometry | Initial velocity | Length | Column collapse height | |
| | | Samples of 1870 eruption | 150 a 200 m/s | 4–8 km | 1500 m | |
| SCENARIO 3 | Plinian eruption Volume: 2.5–5 $km^3$ Eruptive column height: > 20 km VEI > 3 | Volume | Diameter | | Volume | Volume |
| | | 2–4 $km^3$ | > 0.5 m | | 0.5–1 $km^3$ | 9–11 × $10^6$ $m^3$ (water + sediments) |
| | | Eruptive column height | Density | | Bed friction | Sediment input areas |
| | | 15–35 km | Andesite/Dacite 2500–2800 $kg/m^3$ | | | Ceboruco slopes + SMO |
| | | Granulometry | Initial velocity | | Column collapse height | |
| | | Samples of plinian eruption Jala | 150 a 200 m/s | | 1500 m | |
| Modelling computer codes to reproduce volcanic phenomena | | Tephra 2 (Bonadonna et al., 2014) Hazmap (Macedonio et al., 2005) | Eject! Code (Mastin, 2001) | Etna Lava Flow Model (Damiani et al., 2006) | Titan2D (Patra et al., 2005; Sheridan et al., 2005) | Flo-2D (O'Brien et al., 1993) LaharZ (Schilling, 1998) |

#### *Scenario 3 (large magnitude, VEI > 3)*

Explosive Plinian eruption similar to the CE 1000 Jala eruption involving a magma volume ranging between 2.5 and 5 $km^3$. Such an eruption could produce an eruptive column rising > 15 km high and generate large volumes of pyroclastic material. Pyroclastic flows and surges would be associated with collapse of the eruption column. It is considered that this type of eruption would originate within the central summit crater. Additionally, lahars would occur simultaneously or later during subsequent rain periods, both on the slopes of the volcano itself and on steep slopes of the nearby mountainous Sierra Madre Occidental, where ash and pumice lapilli would accumulate.

## Discussion and conclusions

The project "Evaluation of volcanic hazards of Ceboruco volcano (Nayarit)", funded by Mexico's *CFE*, has allowed the synthesizing of relevant geologic information necessary for the construction of a volcanic hazard map for Ceboruco, one of the 5 most active volcanoes in Mexico, just after Colima and Popocatépetl volcanoes. The hazard map is presented in the subsequent part II of the present work (Sieron et al., 2019). Due to its location on the western edge of the TMVB and its current lack of eruptive activity, Ceboruco volcano has not received much attention since the major works on its eruptive history of Nelson (1980) and follow-up work of Gardner,

Browne and Chertkoff (Nelson, 1986; Gardner and Tait, 2000; Browne and Gardner, 2004; Chertkoff and Gardner, 2004). Nevertheless, Ceboruco was classified as one of the most hazardous and risky active volcanoes in Mexico (CENAPRED, 2001) due to its historical activity and the young cataclysmic Plinian eruption only a thousand years ago, as well as poor monitoring. The first step towards hazard assessment, therefore, was the preparation of a hazard map.

Establishing eruptive scenarios based on Ceboruco's eruptive history represents the basis for the hazard map. Ceboruco has experienced numerous eruptions with a large variety of styles separated by periods of repose of varying duration. Only one violent high-magnitude Plinian eruption is documented in its stratigraphic record. The general observation made by volcanologists since the 1970's (e.g. Smith, 1979; Sparks, 1978) might also apply to Ceboruco as already pointed out by Nelson (1980): Short repose times lead to non-explosive or mildly explosive small-volume eruptions, while long repose times are followed by magma evolution during storage in upper crustal levels leading to violent voluminous explosive eruptions such as the ~CE 1000 Plinian Jala eruption which occurred after a repose time of ~ 40,000 years.

Based on Ceboruco's stratigraphic record, we have identified three main different scenarios (Table 5). *Scenarios 1 and 2* are the most probable and the worst-case *Scenario 3* (Plinian eruption) is the least likely for this volcano. Considering that Ceboruco has been in a state of repose for almost 150 years (since 1875), not only *Scenario 1*, but also *Scenario 2* might be likely to occur, in case of renewed eruptive activity in the near future.

It is understandable that the establishment of these three hazard scenarios is based on few eruptions (especially for scenarios 2 and 3). The change of predominantly effusive eruptions to more violent explosive eruptions and longer repose periods makes Ceboruco volcano difficult to predict, compared to volcanoes like Colima with more cyclic activity or like Popocatépetl, and even Pico de Orizaba volcano, with more longer and well known eruptive histories. Nevertheless, we consider that the established hazard scenarios cover all observed eruptive styles and are therefore representative.

The data assigned to the parameters that characterize each volcanic phenomenon for the different considered scenarios (Table 5) were employed as input data for the simulation process, to firstly reproduce the range of the volcanic products of known eruptions (calibration) and latter to stablish the areas that could be impacted during future eruptions of different magnitude. The simulation software (Table 5) used was Tephra2 and Hazmap to simulate ashfall processes, the Eject! code for the simulation of ballistic fragments, Titan2D to simulate pyroclastic flows and surges (with the energy cone module), and LaharZ and Flo2D codes for lahars (Table 5). Selected results of simulations led to the construction of specific hazard maps for each volcanic phenomenon, of eruptive scenario hazard maps and finally to the preparation of the general hazard map of Ceboruco volcano (digital and print versions). The detailed methodologies and the mentioned products were recently published in Sieron et al. (2019) Natural Hazards paper.

The occurrence of at least 28 monogenetic volcanoes, including mostly scoria cones and domes, but also two explosion craters with documented initial phreatomagmatic phases in the surroundings of Ceboruco, entails a considerable additional hazard for the surrounding population. A detailed study characterizing the two volcanoes with phreatomagmatic phases is currently in progress. Hazard assessment taking into account not only the main edifice but also these surrounding monogenetic volcanoes is highly desirable and should be undertaken in the near future.

The general hazard map of the Ceboruco volcano, as well as the technical report on its construction have also been published in Spanish language by the Geophysics Institute of the UNAM (Ferrés et al., 2019) with the aim of constituting useful tools for dissemination of the volcanic hazards in western Mexico. Likewise, the information layers of the map will soon be included in the National Risk Atlas of the National Center of Disaster Prevention (CENAPRED).

**Acknowledgements**

This work is part of the project "*Evaluación del peligro volcánico del volcán Ceboruco (Nayarit), con énfasis en su posible impacto sobre la infraestructura de la Comisión Federal de Electricidad*" (Convenio CFE-800720929), funded by the Comisión Federal de Electricidad. R. Constantinescu was financed through a DGAPA-UNAM postdoctoral fellowship. Archaeologists Raul Barrera Rodríguez and José Carlos Beltran Medina (INAH) provided useful information on the pre-Hispanic cultures of the study area in Nayarit. SPOT satellite images were obtained through the collaborative project between the Universidad Autónoma del Estado de México and the Mexican Service of Agriculture and Fishing (SIAP)-ERMEX through the "*Airbus Defense & Space*" license. We are also thankful to the editor and reviewers, who helped to improve the manuscript.

**Authors' contributions**

KS and DF – major contributor in writing the manuscript (+field work) and defining hazard scenarios. CS – head of the project indicated in acknowledgement section (financial support of all actions leading to the present paper); major contributions in manuscript correction; collaborator during field work. LC – lahar and pyroclastic flows specialist – collaborated during field work and deposit descriptions, helped identifying parameters and undertook simulations. LC – parameter selection and major work on ash fallout scenarios and section. GG – parameter selection and major work on lava flow scenarios and section. RC – parameter selection and major work on pyroclastic flow section. HB – major contribution on lava flow scenarios through field work and paleomagnetic dating of ceboruco lava flows. JAF – field work; major contributions on geologic-hydrologic backround, monogenetic volcanoes in the surroundings; abundant lab work. KGZ – major contributions in map edition, GIS work and lab work. All authors read and approved the final manuscript.

**Funding**

This work is part of the project "*Evaluación del peligro volcánico del volcán Ceboruco (Nayarit), con énfasis en su posible impacto sobre la infraestructura de la Comisión Federal de Electricidad*" (Convenio CFE-800720929), funded by the Comisión Federal de Electricidad, which ended in 2017 (last funds spent in 2018). The funding body has/had no role in the design of the study and collection, analysis, and interpretation of data and in writing the manuscript,

other than provide means to pay expenses during field work, analyses, and salaries and equipment used.
R. Constantinescu was financed through a DGAPA-UNAM postdoctoral fellowship.

### Availability of data and materials
All data generated or analyzed during this study are included in this published article.

### Competing interests
The authors declare that they have no competing interests.

### Author details
[1]Centro de Ciencias de la Tierra, Universidad Veracruzana, Lomas del Estadio s/n, Zona Universitaria, C.P. 91090 Xalapa, Mexico. [2]Departamento de Vulcanologia, Instituto de Geofísica, UNAM, Mexico City, Mexico. [3]Centro de Geociencias, UNAM, Juriquilla Querétaro, Mexico. [4]Geoscience Center, University of South Florida, Tampa, USA. [5]Centro de Investigación en Geografía y Geomática (CentroGeo), Mexico City, Mexico. [6]CNR - Istituto per la Dinamica dei Processi Ambientali - sez. di Milano, Milan, Italy.

Received: 30 May 2019 Accepted: 16 October 2019
Published online: 27 December 2019

### References
Allan JF. Geology of the northern Colima and Zacoalco grabens, southwestern Mexico: late Cenozoic rifting in the Mexican volcanic belt. Geol Soc Am Bull. 1986;97:473–85.
Banda L. Breves noticias del Volcán del Ceboruco. Bol Soc Geogr Estadíst Rep Mex (segunda época) III. 1871:26–34.
Barrera R. Entre ríos y montañas sagradas: Arqueología en El Cajón. Ciudad de México, INAH, México: Nayarit. Publicaciones del Templo Mayor; 2006. 95 pp.
Barrera T. Zonas mineras de los estados de Jalisco y Nayarit. Bol Inst Geol Mex. 1931;51:5–46.
Bell B. Archaeology of Nayarit, Jalisco, and Colima. In: Handbook of Middle American Indians 11; 1971. p. 694–753.
Böhnel H, Pavón-Carrasco FJ, Sieron K, Mahgoub AN. Palaeomagnetic dating of two recent lava flows from Ceboruco volcano, western Mexico. Geophys J Int. 2016;207(2):1203–15.
Bonadonna C, Connor L, Connor CB, Courtland LM (2014) Tephra2, https://vhuborg/resources/tephra2, last access: Dec 2017.
Browne BL, Gardner JE. The nature and timing of caldera collapse as indicated by accidental lithic fragments from the AD 1000 eruption of Volcán Ceboruco, Mexico. J Volcanol Geoth Res. 2004;130:93–105.
Browne BL, Gardner JE. Transport and deposition of pyroclastic material from the ~1000 AD caldera-forming eruption of Volcán Ceboruco, Nayarit, Mexico. Bull Volcanol. 2005;67(5):469–89.
Caravantes A. El Ceboruco. La Naturaleza. Periódico Científico de la Sociedad Mexicana de Historia Natural, vol. 1. Mexico: Imprenta de Ignacio Escalante; 1870. p. 248–52.
Carey S, Sparks RSJ. Quantitative models of the fallout and dispersal of tephra from volcanic eruption columns. Bull Volcanol. 1986;48(2–3):109–25.
Centro Nacional de Prevención de Desastres (CENAPRED). Diagnóstico de peligros e identificación de riesgos de desastres en México. In: Atlas Nacional de Riesgos de la República Mexicana. México: Coordinación Nacional de Protección Civil, Secretaría de Gobernación; 2001. 225 pp.
Centro Nacional de Prevención de Desastres (CENAPRED). Monitoreo hidrogeoquímico del volcán Ceboruco 2014, unpublished internal report; 2016. p. 22.
Chertkoff DG, Gardner JE. Nature and timing of magma interactions before, during, and after the caldera-forming eruption of volcán Ceboruco, Mexico. Contrib Mineral Petrol. 2004;146:715–35.
Chevrel MO, Siebe C, Guilbaud MN, Salinas S. The AD 1250 El Metate shield volcano (Michoacán): Mexico's most voluminous Holocene eruption and its significance for archaeology and hazards. The Holocene. 2016;26(3):471–88.
Connor CB, Connor LJ. Estimating spatial density with kernel methods. In: Connor C, Chapman N, Connor L, editors. Volcanic and Tectonic Hazard Assessment for Nuclear Facilities. Cambridge: Cambridge University Press; 2009. p. 331–43.
Connor LJ, Connor CB, Meliksetian K, Savov I. Probabilistic approach to modeling lava flow inundation: a lava flow hazard assessment for a nuclear facility in Armenia. J Applied Volcanol. 2012;1(1):3.
Damiani ML, Groppelli G, Norini G, Bertino E, Gigliuto A, Nucita A. A lava flow simulation model for the development of volcanic hazard maps for Mount Etna (Italy). Comput Geosci. 2006;32(4):512–26.
Ciudad Real A de (1976) Tratado curioso y docto de las grandezas de la Nueva España. J. Gurría Lacroix (Ed) Vol II (first edition, Madrid 1872), UNAM, México, 482 pp.
Arregui DL de (1946) Descripción de la Nueva Galicia. Van Horne J. (Ed), Escuela de Estudios Hispano-Americanos, Sevilla, Spain, 161 pp.
Espinasa-Pereña R, Nieto-Torres A, Hernández A, Castañeda E. Diagnóstico de los volcanes activos a monitorear por el Servicio Vulcanológico Nacional, Internal report, Subdirección de Riesgos Volcánicos, Dirección de Investigación, Centro Nacional de Prevención de Desastres, Ciudad de México, México; 2015. 227 pp.
Espinasa-Pereña R (2018) Evaluación del riesgo relativo de los volcanes en México. Abstract in VIII Foro Internacional: Los volcanes y su impacto, Arequipa (Perú). http://repositorio.ingemmet.gob.pe/handle/ingemmet/1441
Ferrari L, Conticelli S, Vaggeli G, Petrone CM, Manetti P. Late Miocene volcanism and intra-arc tectonics during the early development of the trans-Mexican Volcanic Belt. Tectonophys. 2000b;318:161–85.
Ferrari L, López-Martínez M, Rosas-Elguera J. Ignimbrite flare-up and deformation in the southern Sierra Madre occidental, western Mexico: implications for the late subduction history of the Farallón plate. Tectonics. 2002;21(4):17–24.
Ferrari L, Nelson SA, Rosas-Elguera J, Aguirre-Díaz G, Venegas-Salgado S. Tectonics and volcanism of the western Mexican Volcanic Belt. In: Aguirre-Díaz G, Aranda-Gómez J, Carrasco-Núñez G, Ferrari L, editors. Magmatism and tectonics in central and northwestern Mexico-a selections of the 1997 IAVCEI general assembly excursions. Mexico: Instituto de Geología, Universidad Nacional Autónoma de México; 1997. p. 85–29.
Ferrari L, Pasquaré G, Venegas S, Castillo D, Romero F. Regional tectonics of western Mexico and its implications for the northern boundary of the Jalisco block. Geofis Int. 1994;33:139–51.
Ferrari L, Petrone CM, Francalanci L, Tagami T, Eguchi M, Conticelli S, Manetti P, Venegas-Salgado S. Geology of the San Pedro-Ceboruco Graben, western trans-Mexican Volcanic Belt. Rev Mex Cienc Geol. 2003;20:165–81.
Ferrari L, Rosas-Elguera J, Delgado-Granados H. Late Miocene to quaternary extension at the northern boundary of the Jalisco block, western Mexico: the Tepic-Zacoalco rift revisited. Geol Soc Amer Spec Paper. 2000a;334:41–64.
Ferres D, Sieron K, González Zuccolotto K. Constantinescu R, Agustin Flores J, Siebe C, Capra L, Connor L, Connor CB, Memoria Técnica del mapa de peligros del volcán Ceboruco (Nayarit). Serie Monografías, 24. Institute of Geophysics, UNAM. 2019. ISBN 978-607-30-1919-4. Mexico City, México.
Frey MH, Lange RA, Hall CM, Delgado-Granados H. Magma eruption rates constrained by $^{40}Ar/^{39}Ar$ chronology and GIS for the Ceboruco-San Pedro volcanic field, western Mexico. Geol Soc Amer Bull. 2004;116(3/4):259–76.
Fuchs CWC. Bericht über die vulkanischen Erscheinungen des Jahres 1870. N Jahrb Mineral Geol Palaeont. 1871:148–61.
García S. Una visita al pueblo de San Cristóbal. Viaje al Ceboruco. In: Informe y colección de artículos relativos a los fenómenos geológicos verificados en Jalisco en el presente año y en épocas anteriores, Tomo II, tipografía de S. Banda, Guadalajara; 1875. 354 pp.
Gardner JE, Tait S. The caldera-forming eruption of Volcán Ceboruco, Mexico. Bull Volcanol. 2000;62:20–33.
Global Volcanism Program (GVN), Smithsonian Institution, last access: Sept 2017, https://volcano.si.edu/volcano.cfm?vn=341030
González-Barajas L, Beltrán-Medina JC. Proyecto de salvamento arqueológico autopista Jala-Compostela km 0+000 al 27+000. Cuauhtémoc: Instituto Nacional de Antropología e Historia (INAH); 2013. 30.
Iglesias M, Bárcena M, Matute JI. El Ceboruco. Anales del Ministerio de Fomento de México 1; 1877. p. 168–96.
INEGI, National Census 2010, [online] Available at: http://www.beta.inegi.org.mx/app/biblioteca/ficha.html?upc=702825002096, last access: Dec 2017.
Kunhardt F. Der Vulkan Ceboruco in México. Petermann's Geograph Mitt 16; 1870. p. 426–9.
Lacroix A. La Montagne Pelée après ses éruptions. Paris: Masson; 1904. 662 pp.
LeBas MJ, LeMaitre RW, Streckeisen A, Zanettin B. A chemical classification of volcanic-rocks based on the total alkali-silica diagram. J Petrol. 1986;27(3):745–50.
Luhr J, Nelson S, Allan J, Carmichael ISE. Active rifting in southwestern Mexico: manifestation of an incipient eastward spreading-ridge jump. Geology. 1985;13:54–7.

Macedonio G, Costa A, Longo A. A computer model for volcanic ash fallout and assessment of subsequent hazard. Comput Geosci. 2005;31(7):837–45.
Mastin LG (2001) A simple calculator of ballistic trajectories for blocks ejected during volcanic eruptions, Unite States Geological Survey, Open-File Report 01–45, 16 pp, http://pubs.usgs.gov/of/2001/0045
McNutt SR. Seismic monitoring. In: Sigurdsson H, editor. Encyclopedia of volcanoes. San Diego: Academic Press; 2000. p. 1095–119.
Nelson SA. Geology and petrology of Volcán Ceboruco, Nayarit, Mexico. Geol Soc Amer Bull. 1980;91:2290–431.
Nelson SA. Geología del Volcán Ceboruco, con una estimación de riesgos de erupciones futuras. Rev Mex Cienc Geol. 1986;6:243–58.
Newhall CG, Self S. The volcanic explosivity index (VEI): an estimate of explosive magnitude for historical volcanism. J Geophys Res. 1982;87-C2:1231–8.
Nieto-Obregón J, Urrutia-Fucugauchi J, Cabral-Cano E, Guzmán de la Campa A. Listric faulting and continental rifting in western Mexico – a paleomagnetic and structural study. Tectonophys. 1992;208:365–76.
O'Brien J, Julien P, Fullerton W. Two-dimensional water flood and mudflow simulation. J Hydraul Eng-ASCE. 1993;119:244–61.
Ordóñez ME. Itinerarios geológicos. In: Aguilera JG, editor. Bosquejo geológico de México: Oficina Tipografía de la Secretaría de Fomento; 1896. 270 pp.
Palacio R. Memoria de la comisión exploradora del volcán del Ceboruco- Anales del Ministerio de Fomento de México 1; 1877. p. 115–67.
Patra A, Bauer A, Nichita CC, Pitman EB, Sheridan MF, Bursik MI, Rupp B, Webber A, Stinton AJ, Namikawa L, Renschler C. Parallel adaptive numerical simulation of dry avalanches over natural terrain. J Volcanol Geoth Res. 2005;139:1–21.
Petrone CM. Relationship between monogenetic magmatism and stratovolcanoes in western Mexico: the role of low-pressure magmatic processes. Lithos. 2010;119:585–606.
Petrone CM, Tagami T, Francalanci L, Matsumura A, Sudo M. Volcanic system in the San Pedro-Ceboruco graben (Nayarit, Mexico) in the light of new K-Ar geochronological data. Geochem J. 2001;35:77–88.
Rodríguez-Uribe MC, Núñez-Cornú FJ, Nava FA, Suárez-Placencia C. Some insights about the activity of the Ceboruco volcano (Nayarit, Mexico) from recent seismic low-frequency activity. Bull Volcanol. 2013;75:755–67.
Rosas-Elguera J, Ferrari L, Garduño-Monroy VH, Urrutia-Fucugauchi J. Continental boundaries of the Jalisco block and their influence in the Pliocene-quaternary kinematics of western Mexico. Geology. 1996;24(19):921–4.
Sánchez JJ, Núñez-Cornú FJ, Suárez-Plascencia C, Trejo-Gómez E. Seismicity at Ceboruco volcano, México. Seism Res Lett. 2009;80:823–30.
Schilling SP. GIS programs for automated mapping of lahar-inundation hazard zones. Vancouver, Washington: USGS Open-files; 1998. p. 98–638.
Sheridan MF, Stinton AJ, Patra AK, Bauer AC, Nichita CC, Pitman EB. Evaluating TITAN2D mass-flow model using the 1963 little Tahoma peak avalanches, Mount Rainier, Washington. J Volcanol Geoth Res. 2005;139(1–2):89–102.
Sieron K. Historia eruptiva, volúmenes emitidos y composición geoquímica e isotópica (sistemas Nd, Sr y Pb) del Volcán Ceboruco y edificios monogenéticos contiguos. Estado de Nayarit. PhD thesis: UNAM; 2009. p. 152.
Sieron K, Böhnel H, Pavón-Carrasco FJ. The last 1000 years of the eruptive history of Ceboruco volcano (Nayarit, Mexico) – new contributions based on paleomagnetic dating. Abstract 26th IUGG general assembly, Prague, Czech Republic; 2015.
Sieron K, Ferres D, Siebe C, Constantinescu R, Capra L, Connor C, Connor L, Groppelli G, González Zuccolotto K. Ceboruco hazard map part II – Modelling volcanic phenomena and construction of the general hazard map. Natural Hazards. Online first (29/01/2019). 2019. https://doi.org/10.1007/s11069-019-03577-5.
Sieron K, Siebe C. Revised stratigraphy and eruption rates of Ceboruco volcano and surrounding monogenetic vents (Nayarit, Mexico) from historical documents and new radiocarbon dates. J Volcanol Geotherm Res. 2008;176:241–64.
Smith RL. Ash flow magmatism. Geol Soc Amer Spec Paper. 1979;180:5–27.
Sparks RSJ. The dynamics of bubble formation and growth in magmas: a review and analysis. J Volcanol Geoth Res. 1978;5:1–37.
Waitz P. "Nubes ardientes" observadas en las erupciones del Jorullo (1759), del Ceboruco (1870) y del Volcán de Colima (1913). Mem Soc Cient Antonio Alzate. 1920;37:267–313.
Zepeda G, Samaniega F, Rodríguez A, Huerta Bahena M, Viart Muñoz M, Becerril RE, Pérez Blas D, Socorro de la Vega D (1993) Informes trimestrales del proyecto "Rescate arqueológico Autopista Ixtlán-Tepic, Nayarit", INAH unpublished report, 29 pp.

## Publisher's Note